# Revised deglaciation history of the Pietrele-Stânişoara glacial complex, Retezat Mts, Southern Carpathians, Romania

Zsófia Ruszkiczay-Rüdiger[1], Zoltán Kern[1], Petru Urdea[2], Régis Braucher[3], Balázs Madarász[4], Irene Schimmelpfennig[3] & ASTER Team[3*]

[1] Hungarian Academy of Sciences (MTA); Research Centre for Astronomy and Earth Sciences, Institute for Geological and Geochemical Research (CSFK-FGI), Budaörsi út 45. 1112 Budapest, Hungary. rrzsofi@geochem.hu; kern@geochem.hu

[2] Department of Geography, West University of Timisoara, Romania. petru.urdea@e-uvt.ro

[3] Aix-Marseille University, CEREGE, CNRS-IRD UM34, BP 80, 13545 Aix-en-Provence Cedex 4, France. braucher@cerege.fr; schimmelpfennig@cerege.fr

[4] Hungarian Academy of Sciences (MTA); Research Centre for Astronomy and Earth Sciences, Geographical Institute, Budaörsi út 45. 1112 Budapest, Hungary, madaraszb@sparc.core.hu

* Maurice Arnold (arnold@cerege.fr), Georges Aumaître (aumaitre@cerege.fr), Didier Bourlès (bourles@cerege.fr), Karim Keddadouche (keddadouche@cerege.fr)

## Abstract

Although geomorphological evidences of Quaternary glaciations of the Southern Carpathians were extensively studied and discussed, the limited number of chronological studies resulted in a poor and controversial knowledge on the age of glaciations and deglaciation of the area. We use new and recalculated in situ produced $^{10}$Be surface Cosmic Ray Exposure (SED) ages of glacial landforms to shed light on the age of the maximum glacial extent and the glacier oscillations during the last deglaciation process on the northern side of the Retezat Mountains. According to our data, the maximum ice extent documented by preserved moraines occurred around $21.0^{+0.8}_{-1.5}$ ka, coincident with the global Last Glacial Maximum (LGM). The deglaciation process during the Lateglacial was characterized by two glacial advances at $18.6^{+0.9}_{-0.8}$ and $16.3^{+0.6}_{-0.6}$ ka. Inferred stabilization date of the penultimate glacial stage at $15.2^{+0.7}_{-0.8}$ ka was closely followed by the abrupt warming at the onset of the Bølling/Allerød documented by a local chironomid-based temperature reconstruction. The last

small glacier advance was dated to $13.5^{+0.5}_{-0.4}$ ka. These recessional/readvance phases agree with other European glacial chronologies.

**Keywords:** cosmic ray exposure dating, cosmogenic $^{10}Be$, LGM, Lateglacial, Carpathians, glacier chronology

## 1. Introduction

In modern studies of landscape evolution, establishing improved chronologies is crucial when aiming at reconstructing past environments. In particular, dating glacio-geomorphic features to investigate the response time of the Earth's cryosphere to climate change is currently of fundamental interest (e.g. Andersen et al., 2006.; Ehlers and Gibbard, 2007; Barker et al., 2009; Denton et al., 2010; Hughes et al., 2013; Rasmussen et al., 2014).

By the end of the 20th century, owing to the previous absence of direct numerical dating methods of glacial landforms, the possibility of routine application of Surface Exposure Dating (SED) revolutionized glacial geochronology (for an overview and references see Balco, 2009). Although several hundred publications have already been released on SED of glacial landforms worldwide, very few studies targeted the Carpathians so far (Kuhlemann et al., 2013a; Makos et al., 2013a,b, 2014; Reuther et al., 2004, 2007; Rinterknecht et al. 2012; Engel et al., 2015; Gheorghiu et al., 2015). However, these studies made the picture somewhat more confusing because the local Last Glacial Maximum (LGM), for instance, apparently occurred in asynchronous timing compared to each other and also to other dated glacial events in Europe (Hughes et al., 2013, Ivy-Ochs et al., 2006, 2009).

The Maximum Ice Extent (MIE) recorded by preserved moraines in Northern and Central Europe (Rinterknecht et al., 2006; Mentlik et al., 2013; Hughes et al., 2015), in the European Alps (Ivy-Ochs et al., 2008) and in the Western Carpathians (Makos et al., 2013a, 2014; Engel et al., 2015) usually coincided with the global Last Glacial Maximum (~23 to 19-18 ka; LGM, Hughes et al., 2013). In the Alps the possible existence of a major glacial advance pre-dating the LGM was described in the Western and Southern Alps (Ivy-Ochs et al., 2008; Hughes et al., 2013) and in the northern foreland of the Austrian Alps (van Husen, 2004). Also, in the Southern Carpathians (Reuther et al., 2004, 2007; Urdea et al., 2011), in the Dinarides (Hughes et al., 2011) and in Anatolia (Akçar et al., 2014), the existence of an earlier, more extensive glaciation was suggested.

During the deglaciation of the Lateglacial (~19-11.7 ka) and Holocene, ice sheets and mountain glaciers re-advanced several times (Rinterknecht et al., 2006; Reuther et al., 2007; Ivy-Ochs et al., 2008; Makos et al., 2013b; Rinterknecht et al., 2012; Kuhlemann et al., 2013a,b).

Critical discussion of leads and lags and of potential coincidences among the glacial chronologies of neighbouring and remote ranges in terms of SED requires common and comparable boundary conditions (such as production rate, half-life and scaling scheme applied during the calculations).

The main objective of this study is to use $^{10}$Be SED dating to disentangle the contradictions in the available South Carpathian glacial chronology. The major question is whether the MIE coincided with the LGM or occurred before, as it was suggested by Reuther et al. (2004, 2007). Another question is whether the timing of LGM and Lateglacial glacier re-advances were synchronous with phases of glacial expansion documented in other European areas.

We recalculate previously published $^{10}$Be data of Reuther et al. (2007) in accordance with the new half-life and production rate of $^{10}$Be, using the same scaling scheme and correction factors for all available data. Besides, a new sample set has been collected in the Retezat Mts to establish a better constrained and extended chronological framework for the area including the MIE moraines and the smallest observed moraine generation, as well.

## 2. The study area

The Carpathians are situated in East Central Europe, between the Alps and the Balkans. South Carpathian glacial landforms have already been recognised by the end of the 19$^{th}$ century and were thoroughly studied ever since (see Urdea and Reuther, 2009 for a detailed revision). Glaciation was heaviest and most azimuthally symmetrical in the Southern Carpathians, with 547 cirques from 631 in total in the Romaian Carpathians (Mindrescu et al., 2010). Pleistocene glaciers descended to 1050-1200 m above sea level (asl) in the highest mountains (Făgăraș, Retezat, Parâng) and several moraine generations of the valleys are indicative of glacier fluctuations (Urdea et al., 2011). Nowadays, no glaciers exist in the Southern Carpathians.

Timing of the past glaciations is under debate: two main theories exist. The first one suggests that the largest glacial advance in the Romanian Carpathians occurred during the penultimate glaciation with one or two glacial advances during the last glacial cycle. This was based on geomorphological and stratigraphical observations (Posea et al., 1974; Posea, 2002; Urdea, 2004). The second one was based on a single radiocarbon age and proposed that all glacial deposits belong to repeated glacier advances during the last glacial phase (Badea et al., 1983; Bălteanu et al., 1998).

The Retezat Mountains are among the highest ranges of the Southern Carpathians reaching the altitude of 2509 m asl (Figs. 1, 2). Although its peak elevation is only the third highest after Făgăraș, (2544 m asl) and Parâng (2519 m asl), the percentage of formerly glaciated areas is the highest (26.8%) and the mean altitude of its end moraines is the lowest (1200 m asl.) in the range (Urdea and Reuther 2009). The area above 1800 m in the Retezat Mts is 116 $km^2$ and the number of glacial cirques is 84 (Mindrescu and Evans, 2014). This high proportion of glaciated areas is because the Retezat Mts, the westernmost high altitude range of the Southern Carpathians (Fig.1) receive more precipitation than the ranges farther east (Mindrescu et al., 2010).

Several moraine generations exist in the Retezat Mts (Urdea, 2000; 2004). Moraines of the most extended glacial stage belong to the M1 or Lolaia glacial advance, with end moraines extending as low as 1035 m asl. Glacial landforms, such as lateral and latero-terminal moraine complexes of this phase currently are forested and have been affected by a certain amount of surface erosion. No glacial landforms have been recognised further down in the area so far (Urdea, 2000, 2004), therefore this moraine is considered to represent the MIE in the study area.

The second largest moraine generation was determined as M2 or Capra-Judele, with well-expressed lateral moraines and terminal moraines extending down to around 1200-1400 m asl. During the deglaciation, several glacier re-advances occurred, which are represented by stadial or re-advance moraines. The most prominent generation of these are located around 1600-1750 m asl. (Fig. 2).

During the M3 or Stevia phase, glaciers retreated to form larger cirque glaciers expressed as prominent latero-terminal moraine complexes and glacial lakes around 1900-2000 m asl.

The smallest glacial phase, the M4 or Beagu is represented as small cirque glaciers close to the rock-walls with latero-terminal moraines around 2100-2150 m asl. Landforms belonging to this phase do not appear in each cirque. They might have been overwritten by later processes or did not develop at all due to unfavourable local conditions.

Granitoid composition of the Retezat Mts. (quartz-bearing granite, granodiorite, gneiss and crystalline schist; Berza et al., 1994) and prominent glacial landforms make it a good candidate for $^{10}$Be SED of the major glacial advances. The first numerical ages were provided by the $^{10}$Be SED study in the Pietrele and Stânişoara valleys, on the northern slope of the Retezat Mts (Reuther et al., 2007). This study became a milestone towards a chronology of the Southern Carpathians' glacial history, although there were no samples from the lowest (M1) moraines. However, in accordance with previous studies, a pre-LGM, early-Würmian (MIS 4) age was proposed for this phase on the basis of pedological investigations. They suggested that the second largest moraine generation (M2) was stabilized during the Lateglacial and had a bimodal age distribution with mean ages of 16.1±1.6 $^{10}$Be yrs (n=11) and 14.4±1.6 $^{10}$Be yrs (n=6). Accordingly, they suggested that there was no major glacier advance during the global LGM in the study area.

Based on two boulder ages bracketing the smaller, M3 glacial phase, it was tentatively assigned to a Younger Dryas (YD) re-advance. Moraines belonging to the smallest, most recent glacial phase (M4) remained undated so far.

In the neighbouring Parâng Mts Urdea and Reuther (2009) discussed five $^{10}$Be SED ages ranging between 16.7±1.5 and 17.9±1.6 ka. Unfortunately, insufficient information regarding both these sample sites and the calculation of their SED age preclude the recalculation and the re-interpretation of these data. A recent $^{10}$Be SED study (Gheorghiu et al., 2015) provided a scattered data set. They suggested a major deglaciation phase of the Parâng Mts at 13.2±0.3 ka with prominent landforms both at 1905 m and 1766 m asl in the Iezer valley. In the neighbouring Gâlcescu valley 14.1±2 ka was suggested as the $^{10}$Be age of a lateral moraine around 2030 m asl, and moraine boulders at 2055 m asl. provided $^{10}$Be exposure ages of 10.2±0.9 ka, suggesting Holocene deglaciation.

## 3. Material and methods

### *3.1.Sample collection*

Sample sites were selected on the basis of field studies and detailed geomorphic mapping (Urdea, 2000) (Fig. 2) considering sample locations of Reuther et al. (2007) as well. The Pietrele and Stânişoara valleys were targeted, similarly to the study of Reuther et al. (2007). However, we collected samples also from the moraines of the most extended (M1) and smallest (M4) glaciations. Besides, a higher lateral moraine of the M2 phase and a prominent terminal moraine of the re-advance phase between the M2 and M3 phases were sampled. Flat-topped or gently dipping boulders of several meters size and in stable position were the main target of our sampling. Samples were collected from moraine boulders at the ridge of the landform, two erratic boulders were lying directly on a whaleback and one sample was collected from a whaleback surface itself (see also Table 1 and Section 4.1). In the case of the degraded and densely forested landforms of the M1 phase, the moraine ridge could not be recognised. Here samples were collected from huge boulders situated far from the currently incising river to minimise the potential risk of mobilization due to moraine erosion and also far from the rockwall to prevent sampling local blocks derived from post-glacial mass movements. We intended to disclose the possibility of post-depositional processes (moraine denudation, block rotation, which can lead to a younger apparent age of the landform), by selecting large boulders with their top 0.6-3.5 m above the moraine surface.

Samples were collected by chipping 1-3 cm thickness of the rock surface using hammer and chisel. Their position was measured by handheld GPS. Topographic shielding and dip of the sampled rock surfaces were measured by a Suunto tandem compass-inclinometer (Table 1). All samples were of granitic lithology containing 20-50 % quartz.

### *3.2. Sample treatment and measurement*

Crushing, mechanical and chemical separation of the quartz and decontamination of atmospheric $^{10}$Be by chemical etching were done in the Cosmogenic Nuclide Sample Preparation Laboratory of Budapest. Subsequent chemical separation of cosmogenic $^{10}$Be was performed at the “Laboratoire National des Nucléides Cosmogéniques” (LN2C) at CEREGE (Aix en Provence, France). Pure quartz was dissolved in HF in the presence of $^{9}$Be carrier (100 mg of 3.025 x $10^{-3}$ g/g $^{9}$Be in-house solution). After substitution of HF by nitric- then hydrochloric acids, ion exchange columns (Dowex 1x8 and 50Wx8) were used to extract $^{10}$Be (Merchel and Herpers, 1999). Targets of purified BeO were prepared for AMS (Accelerator Mass Spectrometry) measurement of the $^{10}$Be/$^{9}$Be ratios at ASTER, the French National AMS Facility (CEREGE, Aix en Provence) (Arnold et al., 2010). These measurements were calibrated against the NIST SRM4325 standard, using an assigned $^{10}$Be/$^{9}$Be ratio of $(2.79\pm0.3)\times10^{-11}$. Analytical uncertainties (reported as 1σ) include uncertainties on AMS counting statistics, uncertainty on the NIST standard $^{10}$Be/$^{9}$Be ratio, an external AMS error of 0.5% (Arnold et al., 2010) and chemical blank measurement. The $^{10}$Be half-life of $(1.387\pm0.01)\times10^{6}$ years (Korschinek et al., 2010; Chmeleff et al., 2010) was used.

### *3.3. Surface exposure age determination*

Determination of a site specific $^{10}Be$ production rate is necessary for the calculation of the SED age of the sampled landforms from the measured $^{10}Be$ concentrations. For this purpose production rates were scaled following Lal (1991)/Stone (2000) with a sea level high latitude production rate (SLHL) of 4.02±0.36 atoms/g $SiO_2$/yr. This production rate is the quadratic mean of recently calibrated production rates in the Northern Hemisphere (Balco et al., 2009; Fenton et al., 2011; Goehring et al., 2012; Briner et al., 2012).

Site specific production rates were corrected for self-shielding using the exponential function of Lal (1991) and an attenuation coefficient of neutrons of 160 g/cm$^2$, and assuming a rock density of 2.7 g/cm$^3$. Topographic shielding, soil and snow shielding factors were calculated using the CosmoCalc 2.2 Excel add-in of Vermeesch (2007) (Table 1, for samples of Reuther et al. (2007) refer to Suppl. Table 1).

Strike and dip of the sampled rock surfaces and the inclination of topographic shielding were measured using hand-held clinometer. The snow shielding was estimated using current observations of three meteorological stations of the Southern Carpathians, representative of different altitudes and wind conditions. Two of them (Cuntu; 1450 m asl; Tarcu; 2180 m asl) are exposed to strong winds and have 150-200 days of snow/year with a maximum average snow thickness 60-70 cm. The position of the third station (Balea Lac; 2038 m asl) is similar to the valleys selected for our study. It is situated in a glacial cirque oriented to the North with 221 days of snow/year with a maximum average snow thickness of 160 cm. Snow cover was estimated for each sample site using the above data differentiating between wind-swept and protected sites and considering the differences in altitude. As a result, a conservative estimate of 30 to 70 cm snow during 4 to 7 months/year (with higher values for locations at higher altitude and in wind sheltered position) was applied for the calculation of snow shielding using a snow density of 0.3 g/cm$^3$. Higher values of past snow cover would increase the calculated $^{10}Be$ exposure ages, and lower values would have the opposite effect. For instance, as an extreme case if snow cover increased by a factor of 2 (which is an unrealistic scenario for the entire exposure history) it might increase the age of the oldest samples by ~3%.

All sample sites were uncovered, except the boulders of the M1 moraine, whose surfaces were covered by up to 5 cm thick layer of peaty soil and moss. Site specific production rates were corrected for this soil cover considering a density of 0.9 g/cm$^3$ during the half of the total exposure duration of the boulders (i.e. during the last ~10.5 ka) (Table1).

At the elevations of the M1 lateral moraine and the lower M2 moraines (~1050m-1600m asl), the surface is covered by fir-spruce-birch forest. The higher M2 moraines (~1600-1800

m) are in the timber line zone, thus covered by scarce and low growth pine. Above ca. 1850 m (M3 and M4 moraines) only dwarf pines are present. According to Cerling and Craig (1994) the effect of an old-growth fir forest on the production rate of cosmogenic $^{3}$He is less than 4%. Plug et al. (2007) also concluded that the shielding effect on cosmic irradiation of an old-growth boreal forest is less than 3%. Differences in tree species and moisture content may result in an even smaller correction of the site specific production rate, therefore $^{10}$Be production rates were not corrected for the vegetation cover effect.

According to thermochronologic and kinematic studies, major uplift and exhumation of the Retezat area occurred during the Tertiary, and Quaternary deformation has been limited in this part of the Southern Carpathians (Matenco and Schmid, 1999; Fügenschuh and Schmid, 2005). On the basis of geodetic data, Zugrăvescu et al. (1998) suggested that the recent uplift rate of the area is up to 1mm/a. Consequently, we calculated the $^{10}$Be exposure ages considering both no uplift correction and a 1 mm/a uplift correction (Table 2).

The sampled rock surfaces exhibited no sign of considerable surface denudation and the edges of the sampled blocks were angular or slightly blunted. For the age calculations, we therefore assessed a maximum rock surface denudation rate of 3 mm/ka based on cosmogenic nuclide data from granitic boulders on an LGM moraine in the northern Swiss foreland (Ivy-Ochs et al., 2004).

$^{10}$Be exposure ages were calculated following Equation (1) and muogenic $^{10}$Be production of Braucher et al. (2011).

eq(1):

$$N_{(x,\varepsilon,t)} = \frac{P_{sp}.\exp\left(-\frac{x}{L_n}\right)\left(1-\exp\left(-\mathrm{t}\left(\frac{\varepsilon}{L_n}+\lambda\right)\right)\right)}{\frac{\varepsilon}{L_n}+\lambda} + \frac{P_{\mu slow}.\exp\left(-\frac{x}{L_{\mu slow}}\right)\left(1-\exp\left(-\mathrm{t}\left(\frac{\varepsilon}{L_{\mu slow}}+\lambda\right)\right)\right)}{\frac{\varepsilon}{L_{\mu slow}}+\lambda} + \frac{P_{\mu fast}.\exp\left(-\frac{x}{L_{\mu fast}}\right)\left(1-\exp\left(-\mathrm{t}\left(\frac{\varepsilon}{L_{\mu fast}}+\lambda\right)\right)\right)}{\frac{\varepsilon}{L_{\mu fast}}+\lambda} + N_0.\exp(-\lambda.t)$$

where N(x,ε,t) is the nuclide concentration function of depth x (g/cm$^2$), denudation rate ε (g/cm$^2$/y) and exposure time t (y). Depths are defined at the centre of the sample. $P_{sp}$, $P_{\mu slow}$, $P_{\mu fast}$ and $L_n$, $L_{\mu slow}$, $L_{\mu fast}$ are the production rates and attenuation lengths of neutrons, slow muons and fast muons, respectively. $L_n$, $L_{\mu slow}$, $L_{\mu fast}$ values used in this paper are 160, 1500 and 4320 g/cm$^2$, respectively (Braucher et al., 2003). $\lambda$ is the radioactive decay constant and $N_0$ is the inherited nuclide concentration. $P_{\mu slow}$, $P_{\mu fast}$ are based on Braucher et al. (2011).

Individual $^{10}$Be exposure ages were grouped according to the mapped glacier advances. Where more than 2 samples belong to a group its coherence was tested using the reduced $\chi^2$ test (Ward and Wilson, 1978). This method enables the identification of outliers until the examined group of data contains only ages that are not significantly different considering associated uncertainties of $\pm 2\sigma$ (95% confidence interval). The age groups that satisfied the reduced $\chi^2$ test were analysed using cumulative probability distribution function (PDF) plots (or camelplots) of the sum of the individual Gaussian distributions (Grey et al., 2014). This method was used to quantify the scattering of boulder SED ages and to provide the most probable $^{10}$Be exposure age of the landform. The curves were produced using the "Camelplot" MATLAB code (Balco, 2009). The $^{10}$Be exposure ages of the moraine stabilization correspond to the most probable values of the studied distributions and the associated uncertainties to the 68% confidence interval ($\pm 1\sigma$) of each PDF plot.

### *3.3. Recalculation of previously published $^{10}$Be exposure age data*

We aim at harmonizing the existing $^{10}$Be SED ages related to glaciations of the Retezat Mountains by a recalculation of published SED ages on a common basis. Accordingly, we used the updated half-life of $^{10}$Be (1.387±0.012) Ma (Korschinek et al., 2010; Chmeleff et al., 2010). This value is lower than the formerly accepted half-life of (1.51±0.06) Ma. Concentrations of the samples published by Reuther et al. (2007) were measured at the ETH tandem facility in Zürich relative to laboratory standard S555 (Kubik and Christl, 2010). These were multiplied by 0.9124 to normalize to the 07KNSTD standard (Balco et al. 2008, updated in 2009 and 2011; Akçar et al., 2011; Schimmelpfennig et al., 2014) which is equivalent to the NIST SRM4325 standard used to calibrate the measurements performed at ASTER, Aix en Provence. The applied SLHL production rate of 4.02±0.36 atoms/g$SiO_2$/yr is also considerably lower than the formerly accepted 5.1 atoms/g$SiO_2$/yr. The site specific production rates were scaled using the polynomials of Stone (2000), uniformly for the new and recalculated sample set.

During the age calculations correction factors of Reuther et al. (2007) were revised and harmonized according to the methodology of the SED age calculations performed in this study. Self-shielding and snow correction were re-calculated using the CosmoCalc (Vermeesch, 2007) with the parameters described above. Uplift rate and rock surface denudation (3.5 mm/a and 5 mm/ka in Reuther et al. (2007), respectively) were decreased to 1.0 mm/a and 3 mm/ka, respectively. Only topographic shielding factors of Reuther et al. (2007) were adopted unchanged, as no raw data were available (Suppl. Table 1). The 10 years lapse between our sample collection (2013) and the reference date (2003) of Reuther et al. (2007) were not taken into account while recalculating the $^{10}$Be exposure ages since they are well within the uncertainty of the SED method, and thus does not affect the conclusions of our study.

## 4. Results

### *4.1. Surface exposure ages*

$^{10}$Be concentrations and calculated SED ages for both new and recalculated samples are presented in Table 2. $^{10}$Be exposure ages calculated with no correction for surface denudation and uplift are considered as minimum age estimates. In the following sections, only $^{10}$Be exposure ages corrected for the assessed 3 mm/a denudation rate and 1 mm/a uplift rate are presented and discussed, as the geomorphology of the area suggests that the scenario considering no uplift and no erosion is unlikely.

***M1 (Lolaia) glacial advance*:** Three boulders (Re13-13, -14, -15) were sampled on the lateral moraine corresponding to the M1 glacial advance, representing the MIE in the Retezat Mts, at an elevation around 1050-1100 m asl. The boulders were of several meter size and in stable position (Table 1, Figs. 2, 3A, B). The $^{10}$Be exposure ages of two boulders suggest an LGM age of the landform (Re13-13 and-14: 21.3±0.8 ka and 20.1±1.0 ka, respectively), while one boulder leads to a significantly younger age (Re 13-15: 15.9±0.9 ka), which suggests post-depositional disturbance (moraine denudation, block rotation) decreasing the $^{10}$Be concentration. Therefore, this sample was discarded as an outlier.

***M2 (Capra-Judele) glacial advance*:** The geomorphological mapping of the study area (Fig. 2) enabled the distinction of a major glacier advance reaching 1200 m asl at the confluence of four valleys and a smaller re-advance phase producing terminal moraines at

1600-1750 m asl (Fig. 2). In the following sections, we discuss the major advance of the Capra-Judele (M2) phase as M2a and the smaller re-advance as M2b. This way, the traditional nomenclature applied to describe the South Carpathian glacial phases by previous authors (Urdea, 2000; Urdea, 2004; Urdea and Reuther, 2009) is still applicable to the study area, with the condition that the Capra-Judele phase includes 2 glacial re-advances in the Northern Retezat Mts. Besides, with the increasing number of chronological data it is possible that in the future the M2b re-advance will be described in other ranges as well.

To date the M2a phase, two erratic boulders (Re13-01 and -03), directly emplaced on a whaleback, and the whaleback itself (Re13-02) were sampled (Figs. 2, 3B,C) on the eastern side of the Stânişoara valley at 1750m and 1770m asl. They yielded $^{10}$Be exposure ages between 19.4±0.6 ka and 18.8±1.0 ka (Table 2). Two boulder samples from an outer moraine ridge (Re13-04, -05), next to the whaleback, provided younger $^{10}$Be ages: 13.6±1.2 ka and 17.6±1.0 ka. In this case, the observed lack of fine-grained material may have resulted in an unstable original position and subsequent toppling of the boulders. Due to the probable effect of post-depositional disturbance, the sample Re13-04 has been skipped from further analysis and data interpretation.

In the Pietrele and the Stânişoara valleys, Reuther et al. (2007) sampled fifteen boulders of lateral moraines (at 1460-1610m asl) and one single boulder on glacially abraded bedrock (SA-03-01; 1718m asl). Besides, they collected one bedrock surface at the transfluence pass between the two valleys (PT-03-16; 2120m asl). We made an attempt to localise these sample sites based on the coordinates published in the original paper, and tentatively plotted them in Fig. 2. The recalculated $^{10}$Be ages are ~14% older in average than the ages published by Reuther et al. (2007; Table 2) and they are in very good agreement with the $^{10}$Be ages calculated for the M2a samples collected for this study. Similarly to the original data set, two age groups can be identified, regardless of the position of the samples along the valley. The recalculated $^{10}$Be ages of the older cluster range from ~18 to ~19.5 ka (11 samples) and those of the younger cluster from ~15.5 to ~17 ka (6 samples). The recalculated and the new sample set will be interpreted and discussed together.

Aiming at the age determination of the M2b re-advance, three large and well embedded boulders were sampled on a well-expressed terminal moraine interpreted as a recessional or stadial moraine situated higher in the Stânişoara valley (1760-1770 m asl) (Figs. 2, 3D, E). Three boulders were sampled at the top of the moraine located in ca. 10 m distance from each other and led to $^{10}$Be exposure ages of 18.9±0.9 ka (Re13-07), 16.3±0.5 ka (Re13-06) and 16.5±0.7 ka (Re13-08).

***M3 (Stevia) glacial advance*:** Two huge boulders were sampled on the lateral moraine in the cirque of the Pietrele valley at 2030 m asl (Re13-11 and -12). These yielded $^{10}$Be exposure ages of 15.0±0.7 ka and 15.4±0.7 ka, respectively (Figs. 2, 4A).

Reuther et al. (2007) targeted a large boulder located downstream from the lower M3 end moraine (PT-03-02; 1851m asl), which has a recalculated $^{10}$Be age of 15.7±0.6 ka. Besides, a very large boulder embedded in the glaciofluvial upfill between two re-advance lobes belonging to the M3 was also sampled to bracket the age of the lowest M3 glacial advance. The recalculated $^{10}$Be age of this boulder (PT-03-02; 1902 m asl) is 13.0±0.5 ka (Figs. 2, 4B), inconsistent with the $^{10}$Be data relevant for the M3 and M4 glacier advances. Therefore this sample was discarded as an outlier and was excluded from further analysis.

***M4 (Beagu) glacial advance*:** Two boulder samples were collected from the lateral part of a well distinguished latero-terminal moraine ridge of a small cirque glacier (Re13-09 and -10; 2140m and 2150m asl) in the Pietrele valley and yielded $^{10}$Be ages of 13.6±0.5 ka and 13.5±0.4 ka (Figs 2, 4C,D). Reuther et al (2007) did not present any samples belonging to the M4 glacial advance (Table 2).

*4.2. Timing of the deglaciation of the Pietrele- Stânişoara valleys*

Due to the small number of data, the samples from the oldest ***M1 (Lolaia) glacier advance*** moraine do not lead to a well expressed peak on the cumulative PDF plot (Fig. 5A). However, its most probable stabilization age of $21.0^{+0.8}_{-1.5}$ ka (Fig. 5B) is significantly different from the data belonging to the next, M2a moraine generation. This result does not support the pre-LGM age of this landform proposed by previous studies based on pedological investigations of lateral moraines at higher position, near the confluence of Pietrele and Stânişoara valleys (Fig. 2) (Reuther et al., 2004, 2007). Their description of this moraine (absence of boulders larger than 30 cm), however, is in sharp contrast with the lateral moraine sampled for this study close to the terminal position of the M1 stage, where it is composed of huge boulders embedded in a finer-grained matrix (Fig. 3A, B). In the absence of the exact location and elevation of the soil pits, it was not possible to judge whether the soil profiles sampled by Reuther et al. (2004, 2007) may represent two distinct glacial phases, or local hydrological conditions and/or if slope processes may be responsible for the difference in their characteristic pedological properties. Our data suggest that the LGM glaciation was well expressed and that glaciers did reach as far down as 1050 m (asl) altitude in the northern side of the Retezat Mts. A pre-LGM glaciation of similar size may have existed, but no morphological expression was found so far and no SED ages are older than LGM.

At the end of the LGM, recession of the valley glaciers of the Retezat Mts initiated. The moraines belonging to the ***M2 (Capra-Judele) phase*** represent several recessional and/or re-advance moraines. Exposure ages of samples from the M2 moraines show a bimodal age distribution with an older peak at ~18.5 ka and a younger peak at ~16.3 ka (Fig. 5A). Most samples belong to the M2a glacier advance (n=22) and only three samples were taken from the M2b. Interestingly, the morphological position of samples belonging to the younger or to the older age cluster are not distinguishable: neighbouring samples from the same landform may belong to one or the other group (Fig. 2; Table 2).

Several interpretations may be invoked to explain this age distribution. One way of interpreting the data is to consider that the moraines were abandoned during the deglaciation following the LGM and that the younger $^{10}$Be exposure ages result from the exhumation and toppling of boulders during subsequent moraine degradation. In this case, the oldest SED age of the landform (19.5±0.7 ka) must also be considered as relevant for the onset of the glacial recession. One would, therefore expect progressively smaller number of $^{10}$Be ages spreading from the oldest age peak towards the younger ages (Putkonen and Swanson, 2003; Balco, 2011) in contrast with our results where the younger $^{10}$Be ages are clustering around a secondary maximum.

A second possible interpretation is that the $^{10}$Be exposure ages older than the younger age cluster have been affected by $^{10}$Be concentrations inherited from previous exposure to cosmic irradiation. This explanation would imply scattered and anomalously old SED ages pre-dating the time of moraine abandonment (Briner, 2009; Balco, 2011), and not a single cluster of old $^{10}$Be ages, as it is for the M2 moraines.

Statistical analyses (MANOVA) of the $^{10}$Be ages belonging to the M2 stage suggest that the two age clusters are significantly different ($p < 0.0005$). Moreover, the ~18.5 ka and the ~16.3 ka $^{10}$Be exposure age clusters passed the reduced $\chi^2$ test (Ward and Wilson, 1978), meaning that ages of each group may belong to the same population (alfa=0.05).

Reuther et al. (2007) suggested that exposure ages of the younger age cluster were affected by post-depositional surface modification under periglacial conditions. Therefore, they accepted the mean SED age of the older age cluster as the time of moraine stabilization. However, they had no data from the M2b moraine generation to support subsequent climate deterioration, which may explain the coherence of the younger age cluster.

Licciardi et al. (2004) and Briner (2009) found similar bimodal age distribution of moraines in the Pine Creek valley, Colorado and in the Wallowa Mts, Oregon. They interpreted the occurrence of these two coherent age clusters from the same moraine as the indication of a composite feature that formed during two successive glaciations of approximately equal extent. However, field observations in the Retezat Mts, does not support two glacier expansions of similar size. The terminal moraine at 1200 m asl could belong to the M2a phase, but the recessional/re-advance moraines at 1600-1750 m asl strongly suggest the past occurrence of a glacial phase with smaller glacier extent.

Accordingly, we suggest that the age of the older, M2a glacier advance corresponds to the oldest $^{10}$Be age measured on the M2 moraine that is 19.5±0.7 ka. Post-LGM glacier recession probably started at $18.6^{+0.9}_{-0.8}$ ka, as indicated by the most probable age of stabilization defined by the M2a age group (n=13; Fig. 5C) after discarding the data that belong to the young age cluster (Table 2). The $16.3^{+0.6}_{-0.6}$ ka $^{10}$Be age of the M2b glacier re-advance was determined by the two boulders of coherent age from the characteristic terminal moraine in the Stânişoara valley (Re13-06 and -08). The $^{10}$Be exposure age of the third boulder was older, similar to the age of the M2a stage, suggesting the presence of inherited $^{10}$Be inventory from the previous glacier advance. The similarity of the most probable SED age of the 2nd peak provided by the cumulative PDF plot considering the entire dataset ($16.3^{+0.8}_{-0.8}$ ka; Fig. 5A) and that of the M2b glacier advance (Fig. 5D) suggests that partial re-mobilization of the older moraines was strongly related to the climate conditions leading to the M2b re-advance or stagnation. This may explain the coherence of the ~16.3 ka age group of the M2 moraine tested by the statistical analysis. The most probable exposure age of the M2b moraine sample set (n=2) suggests that moraine stabilization and Lateglacial deglaciation continued at $16.3^{+0.8}_{-0.8}$ ka (Fig. 5D).

The $^{10}$Be exposure ages of the M2 moraine suggests that deglaciation of the Retezat Mts started by the end of the LGM, at $18.6^{+0.9}_{-0.8}$ ka. Glacier retreat was interrupted by the cold, stadial climate of the Lateglacial (Denton et al., 2010), which resulted in at least one glacier re-advance at $16.3^{+0.6}_{-0.6}$ ka similarly to other European regions (Ivy-Ochs et al., 2006, 2008; Rinterknecht et al., 2006; Federici et al., 2012;.Makos et al., 2014)

The boulder ages (n=2) of the ***M3 (Stevia) glaciation*** are not significantly different and suggest a most probable $^{10}$Be age of moraine stabilization at $15.2^{+0.7}_{-0.8}$ ka (Fig. 5E). This is in agreement with the recalculated $^{10}$Be age of 15.7±0.6 ka of the boulder down-valley from the

M3 end moraine sampled by Reuther et al. (2007; PT-03-03; Fig. 2; Table 2). This moraine represents the last cooling phase before the abrupt warming of the Bølling/Allerød (B/A) interstadial (14.7 ka). Based on the recalculated and new SED age determinations, the YD age of the M3 moraine suggested by Reuther et al. (2007) is untenable.

The youngest peak of the PDF plot (Fig. 5A, F) represents the $13.5^{+0.5}_{-0.1}$ ka most probable $^{10}$Be age of the smallest moraine belonging to the ***M4 (Beagu) glacial advance.*** Accordingly, valley glaciers disappeared from the study area as a result of warming during the B/A warm phase and no sign of glacier advance could be recognised during the YD. The small glacier of the M4 phase most probably could survive the warming of the B/A interstadial due to local cold microclimate induced by the topographic shielding of the cirque wall (Figs 2, 4C, D). Its moraine may then be the result of a short cooling phase within the B/A interstadial (Rinterknecht et al., 2006).

## 5. Discussion

### *5.1. The deglaciation of the Retezat Mountains, regional implications*

Detailed geomorphologic mapping of the Retezat Mts. revealed the existence of several glacial advances between the altitudes of 1050 and 2150 m asl, which were attributed to the Riss and Würm glaciations, with the smallest landforms tentatively placed into the Holocene (Urdea, 2000, 2004; Urdea and Reuther, 2009).

The most extensive glacial advance in the Retezat Mountains (M1) was speculatively assigned to the MIS 4 based on the $^{10}$Be SED of the 2$^{nd}$ largest moraine generation and on a relative chronology derived from pedological investigations (Reuther et al., 2007). However, there were no numerical ages from this moraine generation. In contrast, our new $^{10}$Be ages suggest that the largest mapped glacier advance (M1) in the northern side of the Retezat Mts occurred around ~21 ka, indicating that the local MIE coincided with the LGM. This age corresponds to the cold maximum documented by a recently published biomarker-based quantitative temperature reconstruction from the Black Sea (Sanchi et al., 2014). An older glaciation of similar extent may have existed but its landforms were mostly overrun and wiped out by the LGM glaciations. Later in the LGM glaciers retreated by at least ~1.5-2 km (Figs.2, 6). The presented $^{10}$Be SED ages suggest that a re-advance occurred at 19.5±0.6 ka, and that the moraine was stabilized at $18.6^{+0.9}_{-0.8}$ ka, around the end of the LGM (M2a glacier advance). A second re-advance took place at $16.3^{+0.6}_{-0.6}$ ka (M2b), during the Lateglacial. These $^{10}$Be ages are significantly older than those published by Reuther et al. (2007; 16.1±1.6 ka and 14.4±1.6 ka, respectively). After the recalculations, taking into account the re-evaluation of the $^{10}$Be half-life and of the in situ-produced $^{10}$Be production rate, the $^{10}$Be exposure ages resulting from the $^{10}$Be concentrations measured by Reuther et al. (2007) agree with the new data (Table 2). The most probable $^{10}$Be ages of the M2a and M2b glacier advances presented in this study thus result from the compilation of both the Reuther et al. (2007) and the newly acquired datasets.

An independent record on Lateglacial climate change in the area is the chironomid-inferred mean July air temperature record at Lake Brazi (a lake within the M2b moraine in the Galeş valley; (Fig. 2); Tóth et al., 2012). This record suggested a rapid, 2.8 °C warming from 14.7 to 14.5 ka cal BP at the onset of the B/A interstadial, which probably indicates the most intensive melting period of the M3 glaciers, whose expansion has been $^{10}$Be dated at ~15.2 ka (M3; Fig. 6)

According to pollen and plant macrofossil data and stomata records of Lake Brazi (currently in the coniferous belt of the Retezat Mts), afforestation started around 14.5 ka cal. BP. (Magyari et al., 2011, 2012). The warming at ~14.7 ka, at the beginning of the B/A interstadial or Greenland Interstadial-1 (GI-1), appeared in several records, including the chironomid (Tóth et al., 2012), the vegetation record of the Southern Carpathians (Magyari et al., 2011, 2012), and the temperature signal of branched tetraether lipids of the Black Sea (Sanchi et al., 2014). The $15.2^{+0.7}_{-0.8}$ ka $^{10}$Be exposure age of the M3 moraine is in agreement with these data, suggesting that the warming at the end of the GS-2.1 (or Heinrich Stadial 1; Fig. 6) led to the melting of the last valley glaciers in the area.

Magyari et al. (2009) studied the sediment sequence of two glacial lakes in the Northern Retezat Mts (Lake Brazi, 1740 m asl, and Lake Galeş at 1990 m asl Fig. 2) and suggested that sedimentation in both lakes started at 15.1 to 15.8 ka cal BP, depending on the age-depth modelling. Glacial retreat recorded by the $^{10}$Be chronology suggests that the area of Lake Brazi was deglaciated around $16.3^{+0.6}_{-0.6}$ ka.

Most probably, this lake has formed in a depression created by the melting of a buried ice body within the abandoned moraine. Hence, the onset of lacustrine sediment accumulation at 15.8 ka or even slightly later, is well in agreement with the SED age data. On the other hand, glaciers of the M3 phase extended down to 1890-1930 m asl at $15.2^{+0.7}_{-0.8}$ ka (Fig. 2). Therefore, the onset of lacustrine sedimentation above ~1900 m is not possible before this time. The presented $^{10}$Be data suggest that in the lake Galeş (situated at 1990 m asl), the onset of lacustrine sedimentation must have occurred between the M3 and M4 glacial advances, i.e. between $15.2^{+0.7}_{-0.8}$ ka and $13.5^{+0.5}_{-0.4}$ ka. However, it has to be kept in mind that the age depth modelling of Magyari et al. (2009) was performed for the Lake Brazi only, and that this chronology was then extrapolated to the upper Lake Galeş based on the pollen record.

The abrupt warming at the beginning of the B/A interstadial was followed by a period of relatively stable temperature until the beginning of the Holocene (Tóth et al., 2012). Under the steady climate conditions, small cirque glaciers of the M4 phase could survive the B/A warming for a few hundred years, most probably in favourable microclimate conditions provided by the northerly exposed steep topography. The most probable $^{10}$Be exposure age of the youngest, M4 moraine ($13.5^{+0.5}_{-0.4}$ ka) suggests that: 1) glaciers disappeared by the end of the B/A interstadial and 2) no ice advance occurred in the study area during the YD and Holocene, which is in contrast with suggestions of previous studies. The vegetation change towards a regional opening of the forest cover and expansion of steppe-tundra at 12.8 ka (Magyari et al., 2009, 2011, 2012) may indicate cooling and/or drying of the climate. This cooler and dry climate favoured strong frost weathering processes and, in consequence, the extensive development of the rock glaciers, landforms typically associated to permafrost (Urdea, 1992; Vespremeanu-Stroe et al., 2012). A remarkable change in aquatic ecosystems (diatoms) has also been recorded at the onset of the YD (Buczkó et al., 2012). However, the chironomid-based summer temperature reconstruction suggested only a moderate, <1°C, July mean temperature decrease (Tóth et al., 2012). Considering the above described ecosystem changes during the YD phase together with the absence of glacial advances, we suggest that strong seasonal changes may have affected the Southern Carpathians coupled with a diminished humidity.

### *5.2. The deglaciation of the Retezat Mts. in a European framework*

The LGM (MIS 2) as the period of the most extended glacier advance was described, for instance, in the south-eastern part of the Scandinavian Ice Sheet (Rinterknecht et al., 2006), in the Western Carpathians (Makos et al., 2013a; Engel et al., 2015) and in the European Alps (Monegato et al., 2007; Ivy-Ochs et al., 2008; Federici et al., 2012). However, glacial landforms of the North Alpine foreland in Austria suggest larger glacial extents for the previous glacial phases (Riss: ~MIS6, Mindel: ~MIS12 and Günz: ~MIS16; Van Husen, 2004; Salcher et al; 2010), and in the Western Alps the existence of a major glaciation before the LGM, most probably during the MIS 4, is highly probable (Guiter et al., 2005). According to $^{10}$Be exposure dating of moraines in the Rila Mts, local glacial maximum tends to agree with the global LGM also in the Eastern Balkans (Kuhlemann et al. 2013b), while the penultimate glaciation seems to significantly overtake the LGM advance over the Western Balkans (Hughes et al., 2011). It has to be mentioned that $^{10}$Be SED ages of studies published before 2010 were calculated using the former half-life, standardization and production rate of $^{10}$Be. Here we use several proxies for the age determination of glacial phases, however more accurate comparison of $^{10}$Be SED dated glacial chronologies will be possible only after their recalculation on a common basis.

The study of Reuther et al. (2007) suggested that there was no glacier advance in the Southern Carpathians during the LGM and that the MIE was reached during the MIS 4. The lack of a LGM glacier advance was explained by local aridity during this period of time. Our study made the previously diverse picture less confusing, providing clear evidence of a LGM glacial advance at ~21 ka in the Retezat Mts and suggesting that this was the period of most extensive glaciation in the area (M1 glacier advance).

The Eurasian ice sheets have reached their maximum extent at ~21 ka (Hughes et al., 2015) in good agreement with the $^{10}$Be exposure age of the M1 glacial advance in the Retezat Mts. The most probable $^{10}$Be exposure age of the M2a moraine stabilisation of ~18.6 ka places the post-LGM glacier retreat at the time of the onset of the Northern Hemisphere deglaciation (Denton et al., 2010). The subsequent M2b re-advance at ~16.3 ka is in good agreement with the cold climate spell in Europe between 17 and 15.6 ka, as recorded by several studies (Monegato et al., 2007, Ivy-Ochs et al., 2008, Mentlik et al., 2013; Rinterknecht et al., 2014; Engel et al., 2015). The Lateglacial period of glacial expansion in the Northern Hemisphere is characterised by the largest expansion of sea ice on the North Atlantic and corresponds to the Heinrich Stadial 1 (HS1, ~14.7-18 ka; Barker et al., 2009) or the Greenland Stadial-2.1a (GS-2.1a, ~14.7-17.5 ka; Rasmussen et al., 2014) (Fig. 6).

In the Bohemian Forest, Mentlik et al. (2013) also used new and recalculated $^{10}$Be exposure ages and found that the oldest moraines formed at ~19.5 ka, corresponding to the onset of Northern Hemisphere deglaciation. Subsequent glacier advances in the Bohemian Forest occurred at ~16.2±1.4 ka and ~15.7±0.6 ka, following the global climate oscillations, with a timing similar to that recorded by our SED ages of the M2b and M3 moraines in the Retezat Mts. $^{10}$Be exposure ages around 13.7-14.1 ka of Mentlik et al. (2013) indicate the deposition of the youngest moraines in the middle of the Lateglacial, comparable to our results for the M4 moraine.

A set of low altitude moraines in the Krknoše (Giant) Mts. (Engel et al., 2011, 2014) provided $^{10}$Be moraine exposure ages of ~21.2±0.7 ka, 18.2±0.7 ka, 15.7±0.5, 13.5±0.5 ka and 12.9±0.7 ka, similar to the glacial phases dated by this study in the Retezat Mts. However, Engel et al., (2011) recorded glacier preservation up to 8.4±0.3 ka, which was not observed in the studied valleys of the Retezat Mts.

Rinterknecht et al. (2014) revealed similar timing of the retreat of the Scandinavian Ice Sheet in northeast Germany, with recessional moraine ages established at 15.6±0.6 ka and 13.7±0.7 ka $^{10}$Be ages, similar to the M3 and M4 moraines in the Retezat Mts.

A repeated glacial advance in the Eastern Alps was described using radiocarbon dating and pollen analysis, an approach independent from SED (Monegato et al., 2007). The first pulse was dated at 21-22 ka and the second at 20-17.5 ka, which is well in accordance with the M1 and M2 moraine ages of our study area. They revealed a phase of climate deterioration at 17-15.6 ka by the interruption of afforestation, which may be recorded also in the Southern Carpathians by the repeated glacier advance of the coeval M2b phase.

The revision of the Alpine glacier chronology of Ivy-Ochs et al. (2008) suggested the existence of stagnant glaciers around 19 ka and a post-LGM glacier recession completed at roughly 18 ka. They suggested that several glacier advances (Gschnitz, Clavadel, Daun) occurred between the 18 and 14.7 ka (the beginning of the B/A interglacial). Climate oscillations during this period are well reflected by the existence of several recessional/re-advance moraines during the M2b and M3 phase in the Retezat Mts (Figs. 2, 6). It was suggested that climate oscillations during the B/A interglacial may have led to smaller glacier advances in the Alps, but their morphological evidence was erased by the YD glaciers (Ivy-Ochs et al., 2008). In the Retezat Mts, the M4 moraine may represent one of the B/A climate fluctuations, which was not destroyed due to the absence of later glacier advances in the area.

Maximum extent of the glaciers in the Tatra Mountains, Western Carpathians, was around 26 to 21 ka based on $^{36}$Cl exposure ages (Makos et al., 2013a,b, 2014). $^{10}$Be exposure ages suggest that maximum glacier advance occurred at 22.0±0.8 ka, with a re-advance at 20.5±1.7 ka (Engel et al., 2015). The post LGM deglaciation was interrupted by several oscillations, with a major cold phase around 17 ka. Most intensive post-LGM deglaciation of the High Tatras began around 15.9-15.4 ka, and the studied area became subsequently ice-free during the B/A interstadial followed by a smaller glacier re-advance at 12-12.5 ka, during the YD. The glacier chronology set by our study is well in agreement with the results of Makos et al.

(2013a,b, 2014) and Engel et al., (2015) for the chronology of the deglaciation, except for the YD glacial advance, which was not present in our study area.

On the low altitude Charnagora Ridge of the Ukrainian Carpathians, the mean moraine $^{10}$Be exposure age, depending on the applied $^{10}$Be production rate scaling scheme, was between 12.9 and 13.5 ka (Rinterknecht et al., 2012). Although these ages suggest that moraine stabilization occurred at the beginning or slightly before the YD, the authors proposed a YD age for the moraine deposition. Our data put forward that stabilization of this moraine may have occurred synchronously with the M4 glacial phase of the Retezat Mts.

Finally, in the Făgăraș Mts in the eastern part of the Southern Carpathians, Kuhlemann et al., (2013a) proposed an LGM age for the local MIE, based on the $^{10}$Be SED age of a single boulder dated to 17.4±3.2 ka. For the smaller glacier advances, they calculated SED ages between 15.1±2.4 ka and 12.8±2.0 ka. Unfortunately, the large uncertainties associated to these ages and the lack of replicates (they had only one $^{10}$Be SED age per landform) make these results only a tentative approach, that prevents us from reliably comparing it with our records.

## 6. Conclusions

A glacial chronology constrained by 15 new and 19 recalculated $^{10}$Be surface exposure ages has been established in the northern Retezat Mts. In contrast with the formerly suggested asynchronous glacial chronology, evidence has been delivered that the chronology of the glaciations in the Retezat Mts is synchronous with those of most European areas. The revised chronology strongly supports the existence of an extended glaciation during LGM in the study area, which probably coincided with the maximum glaciation of the area. The first phase of the post-LGM deglaciation occurred after ~18.5 ka, with considerable re-advances at ~16.3 ka and ~15.2 ka, which coincide with the cold climate spell of the Heinrich Stadial 1 (18-14.7 ka; Fig. 6). The interstadial climate during the B/A phase resulted in further glacier recession. Both the cold peak and the phase of the most abrupt warming documented in local (Tóth et al., 2012) and regional (Sanchi et al., 2014) quantitative temperature reconstructions are well reflected in the glacial chronology of the northern Retezat Mts based on the presented $^{10}$Be exposure ages. The possible existence of one short cooling phase interrupting the warming trend was dated at ~13.5 ka by the $^{10}$Be age of a cirque glacier. No glacial landforms attributed to the YD and Holocene could be recognised in the Pietrele and Stânişoara valleys. The record presented in this study is in agreement with the Alpine and North European glacial chronologies, with the exception of the lacking evidence of YD cooling, frequently expressed in the form of glacier advance (Alps, Giant Mts, Western Carpathians).

We also demonstrate that the recalculation of previously published $^{10}$Be exposure ages on a common basis (half-life, production rate, scaling scheme) makes these data comparable with each other and with independent proxies. Such an approach should be applied when comparing datasets which previously appeared to be contradictory or at least asynchronous.

## Acknowledgements

Our research was supported by:

the OTKA PD83610,

the“Lendület” program of the Hungarian Academy of Sciences (LP2012-27/2012),

the MTA-CNRS Hungarian-French bilateral cooperation (NKM-96/2014)

the Bolyai János Scholarship of the Hungarian Academy of Sciences.

New $^{10}$Be measurements have been performed at the French AMS national facility ASTER (CEREGE, Aix en Provence) supported by the INSU/CNRS, the ANR through the "Projets thématiques d’excellence" program for the "Equipements d’excellence" ASTER-CEREGE action, IRD and CEA.

We are grateful to István Hatvani and Gábor Molnár for their help in statistical analysis and Matlab operations, respectively. We are obliged to two Anonymous Reviewers for their useful comments and suggestions, which helped to improve the manuscript. This is contribution No.28. of 2ka Palæoclimatology Research Group.

## References

Akçar, N., Ivy-Ochs, S., Kubik, P.W., Schlüchter, C., 2011. Post-depositional impacts on ‘Findlinge’ (erratic boulders) and their implications for surface-exposure dating. Swiss Journal of Geosciences 104, 445-453.

Akçar, N., Yavuz, V., Ivy-Ochs, S., Reber, R., Kubik, P.W., Zahno, C., Schlüchter, C., 2014. Glacier response to the change in atmospheric circulation in the eastern Mediterranean during the Last Glacial Maximum. Quaternary Geochronology 19, 27-41.

Andersen, K.K., Svensson, A., Rasmussen, S.O., Steffensen, J.P., Johnsen, S.J., Bigler, M., Röthlisberger, R., Ruth, U., Siggaard-Andersen, M.-L., Dahl-Jensen, D., Vinther, B.M., Clausen, H.B., 2006. The Greenland Ice Core Chronology 2005, 15-42 ka. Part 1: constructing the time scale. Quaternary Science Reviews 25, 3246-3257.

Arnold, M., Merchel, S., Bourlès, D.L., Braucher, R., Benedetti, L., Finkel, R.C., Aumaître, G., Gottdang, A., Klein, M., 2010., The French accelerator mass spectrometry facility ASTER: improved performance and developments. Nuclear Instruments and Methods in Physics Research B 268, 1954–1959.

Badea, L., Gâştescu, P., Velcea, V., Bogdan, O., Donisă, I., Dragomirescu, S., Florea, N., Niculescu, G., Popova-Cucu, A., Rosu, A., Sencu, V., 1983. Geografia Romaniei I Geografia fizica . Editura Academiei Republicii Socialiste Romania, Bucuresti, pp. 662.

Balco, G., Stone, J.O., Lifton, N.A., Dunai, T.J., 2008. A complete and easily accessible means of calculating surface exposure ages or erosion rates from $^{10}Be$ and $^{26}Al$ measurements. Quaternary Geochronology 3, 174-195.

Balco, G., 2009. MATLAB Code for Camel Diagrams. http://cosmognosis.wordpress.com/2009/07/13/matlab-code-for-camel-diagrams (February 2013).

Balco, G., 2011. Contributions and unrealized potential contributions of cosmogenic nuclide exposure dating to glacier chronology, 1990–2010. Quaternary Science Reviews 30, 3–27.

Balco, G., Briner, J., Finkel, R.C., Rayburn, J., Ridge, J.C., Schaefer, J.M., 2009. Regional beryllium-10 production rate calibration for late-glacial northeastern North America. Quaternary Geochronology 4, 93-107.

Bălteanu, D., Ielenicz, M., Popescu, N. 1998. Geomorphology of the Romanian Carpathians. New trends and evolutions. Studia Geomorphologica Carpatho-Balcanica 32, 89–109.

Barker, S., Diz, P., Vautravers, M.J., Pike, J., Knorr, G., Hall, I.R., Broecker, W.S., 2009. Interhemispheric Atlantic seesaw response during the last deglaciation. Nature 457, 1097-1102.

Berza, T., Andar, P., Udrescu, C., Macalet, V. 1994. Retezat granitoid pluton (South Carpathians), a geochemical approach. Rom. J. Petrology, 76, 1-18.

Braucher, R., Brown, E.T., Bourlés, D.L., Colin, F. 2003. In situ produced $^{10}Be$ measurements at great depths: implications for production rates by fast muons. Earth and Planetary Science Letters 211, 251-258.

Braucher, R., Merchel, S., Borgomano, J., Bourles, D.L. 2011. Production of cosmogenic radionuclides at great depth: A multi element approach. Earth and Planetary Science Letters 309, 1-9.

Briner, J.P. 2009. Moraine pebbles and boulders yield indistinguishable $^{10}$Be ages: A case study from Colorado, USA. Quaternary Geochronology, 4, 299-305.

Briner, J.P., Young, N.E., Goehring, B.M., Schaefer, J.M., 2012. Constraining Holocene $^{10}$Be production rates in Greenland. Journal of Quaternary Science 27, 2-6.

Buczkó, K., Magyari, E., Hübener, T., Braun, M., Bálint, M., Tóth, M., Lotter, A.F. 2012. Responses of diatoms to the Younger Dryas climatic reversal in a South Carpathian mountain lake (Romania). Journal of Paleolimnology 48, 417-431.

Cerling, T.E., Craig, H., 1994. Cosmogenic $^{3}$He production rates from 39°N to 46°N latitude, western USA and France. Geochimica et Cosmochimica Acta 58, 249-255.

Chmeleff, J., von Blanckenburg, F., Kossert, K., Jakob, J., 2010. Determination of the 10Be half-life by multicollector ICP-MS and liquid scintillation counting. Nuclear Instruments and Methods in Physics Research B 268 (2), 192-199.

Denton, G.H., Anderson, R.F., Toggweiler, J.R., Edwards, R.L., Schaefer, J.M., Putnam, A.E., 2010. The Last Glacial Termination. Science 328, 1652-1656.

Dunai, T., 2001. Influence of secular variation of the magnetic field on production rates of in situ produced cosmogenic nuclides. Earth and Planetary Science Letters 193, 197–212.

Dunai, T.J. 2010. Cosmogenic Nuclides. Principles, Concepts and Applications in the Earth Surface Sciences. Cambridge University Press, New York, pp. 187.

Ehlers, J. Gibbard, P. 2007. The extent and chronology of Cenozoic Global Glaciation. Quaternary International 164-165, 6-20.

Engel, Z., Traczyk, A., Braucher, R., Woronko, B., Křížek, M., 2011. Use of $^{10}$Be exposure ages and Schmidt hammer data for correlation of moraines in the Krkonoše Mountains. Zeitschrift für Geomorphologie N.F. 55 (2), 175-196.

Engel, Z., Braucher, R., Traczyk, A., Léanni, L., AsterTeam, 2014. $^{10}$Be exposure age chronology of the last glaciation in the Krkonoše Mountains, Central Europe. Geomorphology 206, 107-121.

Engel, Z., Mentlík, P., Braucher, R., Minár, J., Léanni, L., AsterTeam, 2015. Geomorphological evidence and$^{10}$Be exposure ages for the Last Glacial Maximum and deglaciation of the Velká and Malá Studená dolina valleys in the High Tatra Mountains, central Europe. Quaternary Science Reviews 124, 106-123.

Federici, P.R., Granger, D.E., Ribolini, A., Spagnolo, M., Pappalardo, M., Cyr, A.J., 2012. Last Glacial Maximum and the Gschnitz stadial in the Maritime Alps according to $^{10}$Be cosmogenic dating. Boreas 41, 277–291.

Fenton, C.R., Hermanns, R.L., Blikra, L.H., Kubik, P.W., Bryant, C., Niedermann, S., Meixner, A., Goethals, M.M., 2011. Regional 10Be production rate calibration for the past 12 ka deduced from the radiocarbon-dated Grotlandsura and Russenes rock avalanches at 69° N, Norway. Quaternary Geochronology 6, 437-452.

Fügenschuh, B., Schmid, S.M., 2005. Age and significance of core complex formation in a very curved orogen: Evidence from fission track studies in the South Carpathians (Romania). Tectonophyiscs 404, 33-53.

Gheorghiu, D.M., Hosu, M., Corpade, C., Xu, S. 2015. Deglaciation constraints in the Parâng Mountains, Southern Romania, using surface exposure dating. Quaternary International (in press) http://dx.doi.org/10.1016/j.quaint.2015.04.059

Goehring, B.M., Lohne, Ø.S., Mangerud, J., Svendsen, J.I., Gyllencreutz, R., Schaefer, J., Finkel, R., 2012. Lateglacial and Holocene $^{10}$Be production rates for western Norway. Journal of Quaternary Science 27, 89-96.

Gosse, J. C. Phillips, F. M. 2001. Terrestrial in situ cosmogenic nuclides: theory and application, Quaternary Science Reviews 20, 1475–1560.

Guiter, F., Triganon, A., Andrieu-Ponel, V., Ponel, P., Hébrard, J-P., Nicoud, G., Beaulieu, J-L., Brewer, S., Guibal, F.. 2005. First evidence of 'in-situ' Eemian sediments on the high plateau of Evian (Northern Alps, France): implications for the chronology of the Last Glaciation. Quaternary Science Reviews 24, 35–47.

Hughes,

Hughes, A. L. C., Gyllencreutz, R., Lohne, Ø. S., Mangerud, J., Svendsen, J. I. 2015. The last Eurasian ice sheets – a chronological database and time-slice reconstruction, DATED-1. Boreas. (In press) 10.1111/bor.12142. ISSN 0300-9483.

Hughes, P.D., Woodward, J.C., van Calsteren, P.C., Thomas, L.E. 2011. The glacial history of the Dinaric Alps, Montenegro. Quaternary Science Reviews, 30, pp. 3393–3412

Hughes, P.D., Gibbard, P.L., Ehlers, J. 2013. Timing of glaciation during the last glacial cycle: evaluating the concept of a global 'Last Glacial Maximum' (LGM). Earth-Science Reviews 125, 171-198.

Ivy-Ochs, S., Schaefer, J., Kubik, P.W., Synal, H.A., Schlüchter, C., 2004. The timing of deglaciation on the northern Alpine foreland (Switzerland). Eclogae geologicae Helvetiae 97, 47–55.

Ivy-Ochs, S., Kerschner, H., Reuther, A., Maisch, M., Sailer, R., Schaefer, J., Kubik, P.W., Synal, H-A., Schlüchter, C. 2006. The timing of glacier advances in the northern European Alps based on surface exposure dating with cosmogenic $^{10}$Be, $^{26}$Al, $^{36}$Cl, and $^{21}$Ne. Geological Society of America, Special Paper 415. 43-60.

Ivy-Ochs, S., Kerschner, H., Reuther, A., Preusser, F., Heine, K., Maisch, M., Kubik, P.W., Schlüchter, C., 2008. Chronology of the last glacial cycle in the European Alps. Journal od Quaternary Science 23, 559-573.

Ivy-Ochs, S., Kerschner, H., Maisch, M., Christl, M., Kubik, P.W., Schlüchter, C. 2009. Latest Pleistocene and Holocene glacier variations in the European Alps. Quaternary Science Reviews, 28, 2137-2149.

Korschinek, G., Bergmaier, A., Faestermann, T., Gerstmann, U.C., Knie, K., Rugel, G., Wallner, A., Dillmann, I., Dollinger, G., von Gostomski, Lierse Ch., Kossert, K., Maitia, M., Poutivtsev, M., Remmert, A., 2010. A new value for the half-life of $^{10}$Be by Heavy-Ion Elastic Recoil Detection and liquid scintillation counting. Nuclear Instruments and Methods in Physics Research B 268 (2), 189-191.

Kuhlemann, J., Dobre, F., Urdea, P., Krumrei, I., Gachev, E., Kubik, P., Rahn, M. 2013a. Last Glacial Maximum Glaciation of the Central South Carpathian Range (Romania). Austrian Journal of Earth Sciences, 106 83-95.

Kuhlemann, J. Gachev, E., Gikov, A., Nedkov, s., Krumrei, I., Kubik P 2013b Glaciation in the Rila Mountains (Bulgaria) during the last glacial maximum. Quaternary International, 293 51–62

Kubik, P., Christl, M., 2010. $^{10}$Be and $^{26}$Al measurements at the Zurich 6 MV tandem AMS facility. Nuclear Instruments and Methods in Physics Research, Section B: Beam Interactions with Materials and Atoms 268, 880e883.

Lal, D. 1991. Cosmic ray labeling of erosion surfaces: in situ nuclide production rates and erosion models, Earth and Planetary Science Letters 104, 424–439.

Licciardi, J.M., Clark, P.U., Brook, E.J., Elmore, D., Sharma, P., 2004. Variable responses of western U.S. glaciers during the last deglaciation. Geology 32, 81–84.

Magyari, E.K., Braun, M., Buczkó, K., Kern, Z., László, P., Hubay, K., Bálint, M., 2009. Radiocarbon chronology and basic characteristics of glacial lake sediments in the Retezat Mts (S Carpathians, Romania): a window to Lateglacial and Holocene climatic and palaeoenvironmental changes. Central European Geology 52, 225-248.

Magyari, E.K., Major, Á., Bálint, M., Nédli, J., Braun, M., Rácz, I., Parducci, L., 2011. Population dynamics and genetic changes of Picea abies in the South Carpathians revealed by pollen and ancient DNA analyses. BMC Evolutionary Biology 11, 66.

Magyari, E.K., Jakab, G., Bálint, M., Kern, Z., Buczkó, K., Braun, M., 2012. Rapid vegetation response to Lateglacial and early Holocene climatic fluctuation in the South Carpathian Mountains (Romania). Quaternary Science Reviews. 35, 116-130.

Makos, M., Nitychoruk, J., Zreda, M., 2013a. Deglaciation chronology and paleoclimate of the Pięciu Stawów Polskich/Roztoki Valley, High Tatra Mountains, Western Carpathians since the Last Glacial Maximum, inferred from $^{36}$Cl exposure dating and glacier–climate modeling. Quaternary International 293, 63–78.

Makos, M., Nitychoruk, J., Zreda, M., 2013b. The Younger Dryas climatic conditions in the Za MnichemValley (Polish High Tatra Mountains) based on exposure-age dating and glacier–climate modeling. Boreas 42 (3), 745–761.

Makos, M., Dzierżek, J., Nitychoruk, J., Zreda, M. 2014. Timing of glacier advances and climate in the High Tatra Mountains (Western Carpathians) during the Last Glacial Maximum. Quaternary Research 82, 1-13.

Matenco, L., Schmid, S., 1999. Exhumation of the Danubian nappes system (South Carpathians) during the early Tertiary: inferences from kinematic and paleostress analysis at the Getic/Danubian nappes contact. Tectonophysics 314, 401-422.

Mentlík, P., Engel, Z., Braucher, T., Léanni, L., Aster Team, 2013. Chronology of the Late Weichselian glaciation in the Bohemian Forest in Central Europe. Quaternary Science Reviews 65, 120-128.

Mindrescu, M., Evans I.S., Cox, N.J., 2010. Climatic implications of cirque distribution in the Romanian Carpathians: Palaeowind directions during glacial periods. Journal of Quaternary Science 25(6), 875–888.

Mindrescu, M., Evans, I.S., 2014. Cirque form and development in Romania: allometry and the buzz-saw hypothesis. Geomorphology, 208, 117-136.

Monegato, G., Ravazzi, C., Donegana, M., Pini, R., Calderoni, G., Wick, L., 2007. Evidence of a two-fold glacial advance during the last glacial maximum in the Tagliamento end moraine system (eastern Alps). Quaternary Research, 68, 284-302.

Plug, L.J., Gosse, J.C., McIntosh, J.J., Bigley, R., 2007. Attenuation of cosmic ray flux in temperate forest. Journal of Geophysical Research 112. doi:10.1029/2006JF000668.

Posea, G., Popescu, N., Ielenicz, M., 1974. Relieful Romaniei. Editura Stiintifica, Bucuresti, pp. 483.

Posea, G., 2002. Geomorfologica Romaniei. Editura Fundatiei Romania de Maine, Bucuresti, pp. 444.

Putkonen, J., Swanson, T., 2003. Accuracy of cosmogenic ages for moraines. Quaternary Research 59, 255–261.

Rasmussen, S.O., Andersen, K.K., Svensson, A.M., Steffensen, J.P., Vinther, B.M., Clausen, H.B., Siggaard-Andersen, M.-L., Johnsen, S.J., Larsen, L.B., Dahl- Jensen, D., Bigler, M., Röthlisberger, R., Fischer, H., Goto-Azuma, K., Hansson, M.E., Ruth, U. 2006 A new Greenland ice core chronology for the last glacial termination. Journal of Geophysical Research 111, D06102, 2006, doi:10.1029/2005JD006079

Rasmussen, S.O., Bigler, M., Blockley, S.P.E., Blunier, T., Buchardt, S.L., Clausen, H.B., Cvijanovic, I., Dahl-Jensen, D., Johnsen, S.J., Fischer, H., Gkinis, V., Guillevic, M., Hoek, W.Z., Lowe, J.J., Pedro, J., Popp, T., Seierstad, I.K., Steffensen, J.P., Svensson, A.M., Vallelonga, P., Vinther, B.M., Walker, M.J.C., Wheatley, J.J., Winstrup, M., 2014. A stratigraphic framework for naming and robust correlation of abrupt climatic changes during the last glacial period based on three synchronized Greenland ice core records. Quaternary Science Reviews 106, 14-28.

Reuther, A., Geiger, C., Urdea, P., Heine, K., 2004. Determining the glacial equilibrium line altitude (ELA) for the Northern Retezat Mts. Southern Carpathians and resulting paleoclimatic implications for the last glacial cycle. Analele Universitatea de Vest din Timisoara, GEOGRAFIE XIV, 11–34.

Reuther, A., Urdea, P., Geiger, C., Ivy-Ochs, S., Niller, H.P., Kubik, P., et al., 2007. Late Pleistocene glacial chronology of the Pietrele Valley Retezat Mountains, Southern Carpathians, constrained by $^{10}$Be exposure ages and pedological investigations. Quaternary International 164–165, 151–169.

Rinterknecht, V.R., Clark, P.U., Raisbeck, G.M., Yiou, F., Bitinas, A., Brook, E.J., Marks, L., Zelčs, V., Lunkka, J.-P., Pavlovskaya, I.E., Piotrowski, J.A., Raukas, A., 2006. The last deglaciation of the southeastern sector of the Scandinavian ice sheet. Science 311, 1449–1452.

Rinterknecht, V., Matoshko, A., Gorokhovich, Y., Fabel, D., Xu, S., 2012. Expression of the Younger Dryas cold event in the Carpathian Mountains, Ukraine? Quaternary Science Reviews 39, 106-114.

Rinterknecht, V., Börner, A., Bourlès, D., Braucher, R., 2014. Cosmogenic $^{10}$Be dating of ice sheet marginal belts in Mecklenburg-Vorpommern, Western Pomerania (northeast Germany). Quaternary Geochronology 19, 42-51.

Salcher, B.C., Hinsch, R., Wagreich, M. 2010. High-resolution mapping of glacial landforms in the North Alpine Foreland, Austria. Geomorphology 122, 283-293.

Sanchi, L., Ménot, G., Bard, E. 2014. Insights into continental temperatures in the northwestern Black Sea area during the Last Glacial period using branched tetraether lipids. Quaternary Science Reviews, 84. 98-108.

Schimmelpfennig, I. Schaefer, J.M., Akçar, N., Koffman, T., Ivy-Ochs, S., Schwartz, R., Finkel R.C., Zimmerman, S., Schlüchter, C. 2014. A chronology of Holocene and Little Ice Age glacier culminations of the Steingletscher, Central Alps, Switzerland, based on high-sensitivity beryllium-10 moraine dating. Earth and Planetary Science Letters 393, 220-230.

Stone, J.O., 2000. Air pressure and cosmogenic isotope production. Journal of Geophysical Research 105 (B10), 23753–23759.

Tóth, M., Magyari, E.K., Brooks, S.J., Braun, M., Buczkó, K., Bálint, M., Heiri, O., 2012. A chironomid-based reconstruction of late glacial summer temperatures in the southern Carpathians (Romania). Quaternary Research 77, 122-131.

Urdea, P., 1992. Rock glaciers and periglacial phenomena in the Southern Carpathians. Permafrost and Periglacial Processes 3, 267-273.

Urdea, P., 2000. Muntii Retezat. Studiu geomorphologic. Editura Academiei, Bucuresti, pp. 272.

Urdea, P., 2004. The Pleistocene glaciation of the Romanian Carpathians. In: Ehlers, J., Gibbard, P.L. (Eds.), Quaternary Glaciations—Extent and Chronology, Part I, 301–308.

Urdea, P., Reuther, A. 2009. Some new data concerning the Quaternary glaciation in the Romanian Carpathians. Geographica Pannonica, 13, 2, 41-52.

Urdea, P., Onaca, A., Ardelean, F., Ardelean, M. 2011. New Evidence on the Quaternary Glaciation in the Romanian Carpathians. Developments in Quaternary Science, Elsevier, Amsterdam, 305-322.

van Husen, D. 2004. Quaternary glaciations in Austria. In: Ehlers, J., Gibbard, P.L. (Eds.), Quaternary Glaciations—Extent and Chronology, Part I, 1-13.

Vermeesch, P., 2007. CosmoCalc: an Excel add-in for cosmogenic nuclide calculations. Geochemistry, Geophysics, Geosystems 8. doi:10.1029/ 2006GC001530 Q08003

Vespremeanu-Stroe, A., Urdea, P., Popescu, R., Vasile, M. 2012. Rock Glacier Activity in the Retezat Mountains, Southern Carpathians, Romania. Permafrost and Periglacial Processes 23, 127–137.

Ward, G. K., Wilson, S. R. 1978. Procedures for Comparing and Combining Radiocarbon Age-Determinations - Critique. Archaeometry, 20, 19-31.

Zugrăvescu, D., Polonic, G., Horomnea, M., Dragomir, V. 1998. Recent vertical crustal movements on the Romanian territory, major tectonic compartments and their relative dynamics. Revue Roumaine de Geophysique, 42. 3-14.

**Figure captions:**

Fig. 1. SRTM-based digital elevation model of the Carpathians and location of the study area (yellow rectangle, Fig. 2). Red dashed lines are the state boundaries. Bp: Budapest; Bu: Bucarest. Mountain ranges mentioned in the text are indicated.

Fig. 2. Digital elevation model (DEM) and glacial landforms of the study area (modified after Urdea, 2000 and Reuther et al., 2007) with sample locations. M1-M4 indicates the position of the terminal moraines of the discussed glacial phases. Coordinates of the DEM: 45.43508N, 22.84447E (top left) and 46.36205N, 22.9384E (bottom right). For location refer to Fig. 1.

Fig. 3. Field images of the lower and middle section of the Pietrele-Stânişoara valleys (M1 and M2 phases).

(A) road-cut in the M1 moraine close to the sample site Re13-15. Note large amount of boulders in the outcrop. (B) Sample site of Re13-14. (C) M2a whaleback (Re13-02) and (D) an erratic boulder on top of the whaleback (Re13-01) at the eastern side of the Stânişoara valley. Dashed yellow line shows the trimline. (E) M2b recessional moraine in the Stânişoara valley looking from north. Red arrow indicates the sampling location. Persons are circled for scale. (F) Sampled boulders on the M2b moraine (Re13-06, -07, -08). For locations of the sample sites see Fig. 2.

Fig. 4. Field images of the upper section of the Pietrele valley (M3 and M4 phases).

(A) Lateral moraine of the M3 glacier advance on the western side of the Pietrele valley. View from the Re13-11 sample site. Persons are circled for scale at the sample location Re13-12. (B) Northward view of the Pietrele valley from an M3 recessional moraine. The M3 terminal moraine and the boulder sampled by Reuther et al. (2007) (PT-03-02) in the outwash plain behind the M3 moraine are well visible. (C) Moraine ridge of the M4 cirque glacier with the sample sites. (D) A close-up of one of the sampled boulders (Re13-09). Its location on the moraine ridge is indicated on the "C" subset image. For locations of the sample sites see Fig. 2.

Fig. 5. Probability distribution functions (PDF) of the $^{10}$Be SED ages of the glacier advances recognised in the study area (Balco, 2009). Thin red curves represent individual boulder SED ages and error with assumed Gaussian distributions; bold black curves represents sum of individual distributions. Red numbers are the most probable SED ages (ka). (A) PDF plot of all samples; (B) PDF plot of the M1 glacier advance; (C) PDF plot of the M2a glacier advance; (D) PDF plot of the M2b glacier advance; (E) PDF plot of the M3 glacier advance; (F) PDF plot of the M4 glacier advance.

Fig. 6. Most probable SED ages of glacier advances (defined by the probability distribution functions of Fig. 5) and lower limit of the extension of glacier tongues defined by the position (elevation asl) of end-moraines (Fig. 2) plotted against the $\delta^{18}$O curve of the NGRIP1 core and the Greenland event chronology on the b2k timescale (Greenland Ice Core Chronology 2005, GICC05, NGRIP1 core, Rasmussen et al., 2006; Andersen et al., 2006). GS: Greenland Stadial, GI: Greenland Interstadial; YD: Younger Dryas; B/A: Bølling/Allerød; HS1: Heinrich Stadial 1.

Figure 1

Click here to download high resolution image

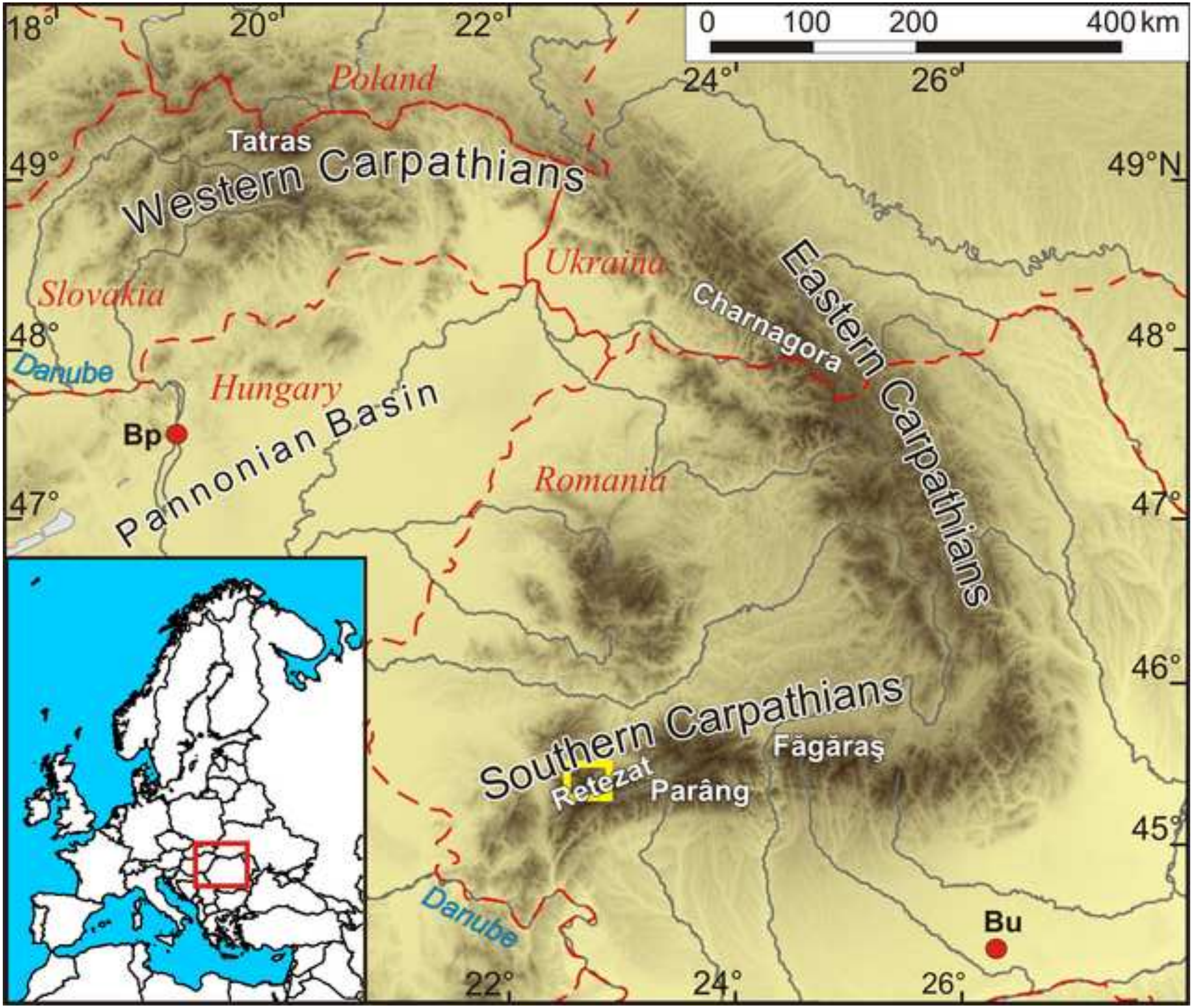

Figure 2

Click here to download high resolution image

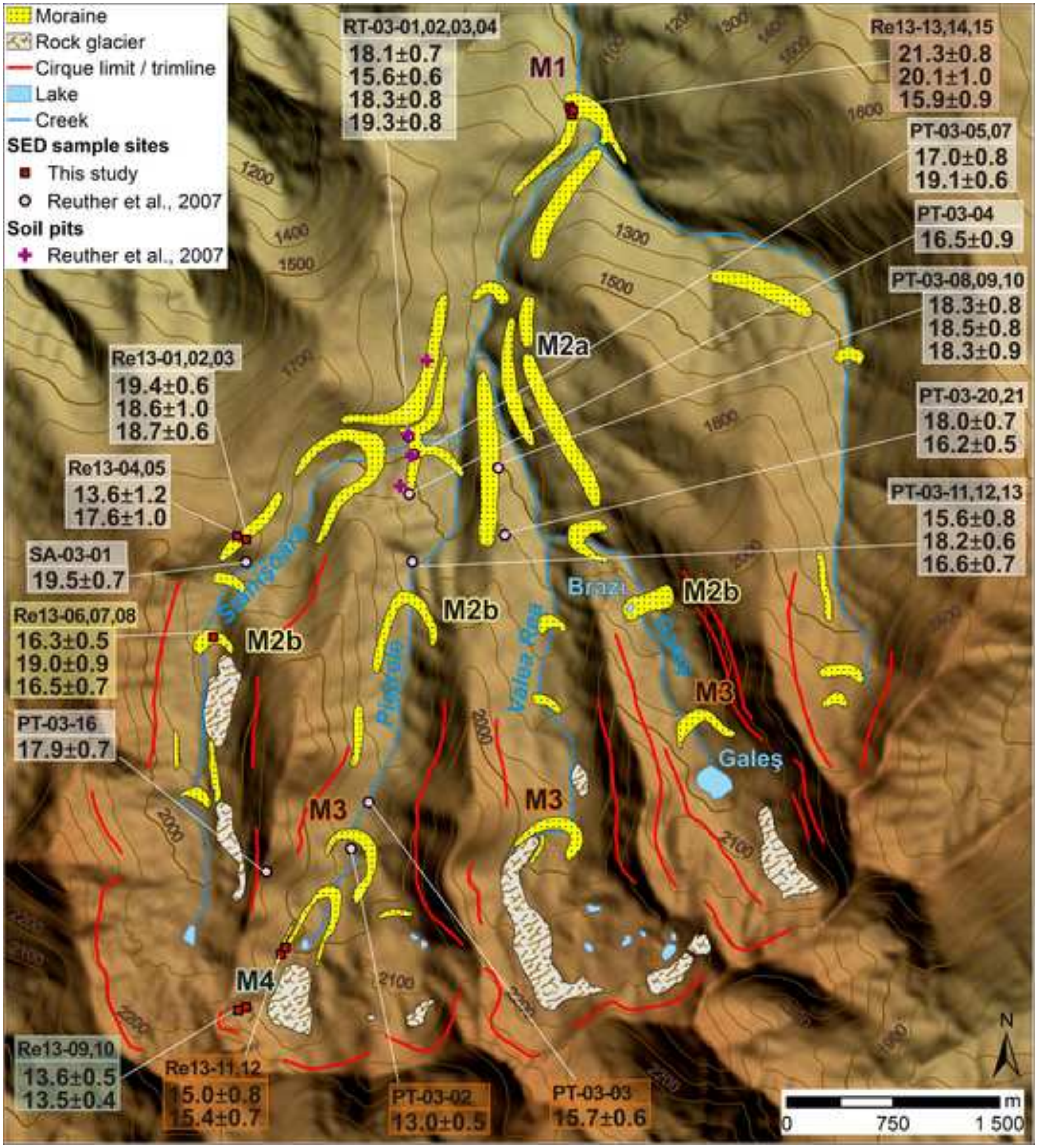

Figure 3
Click here to download high resolution image

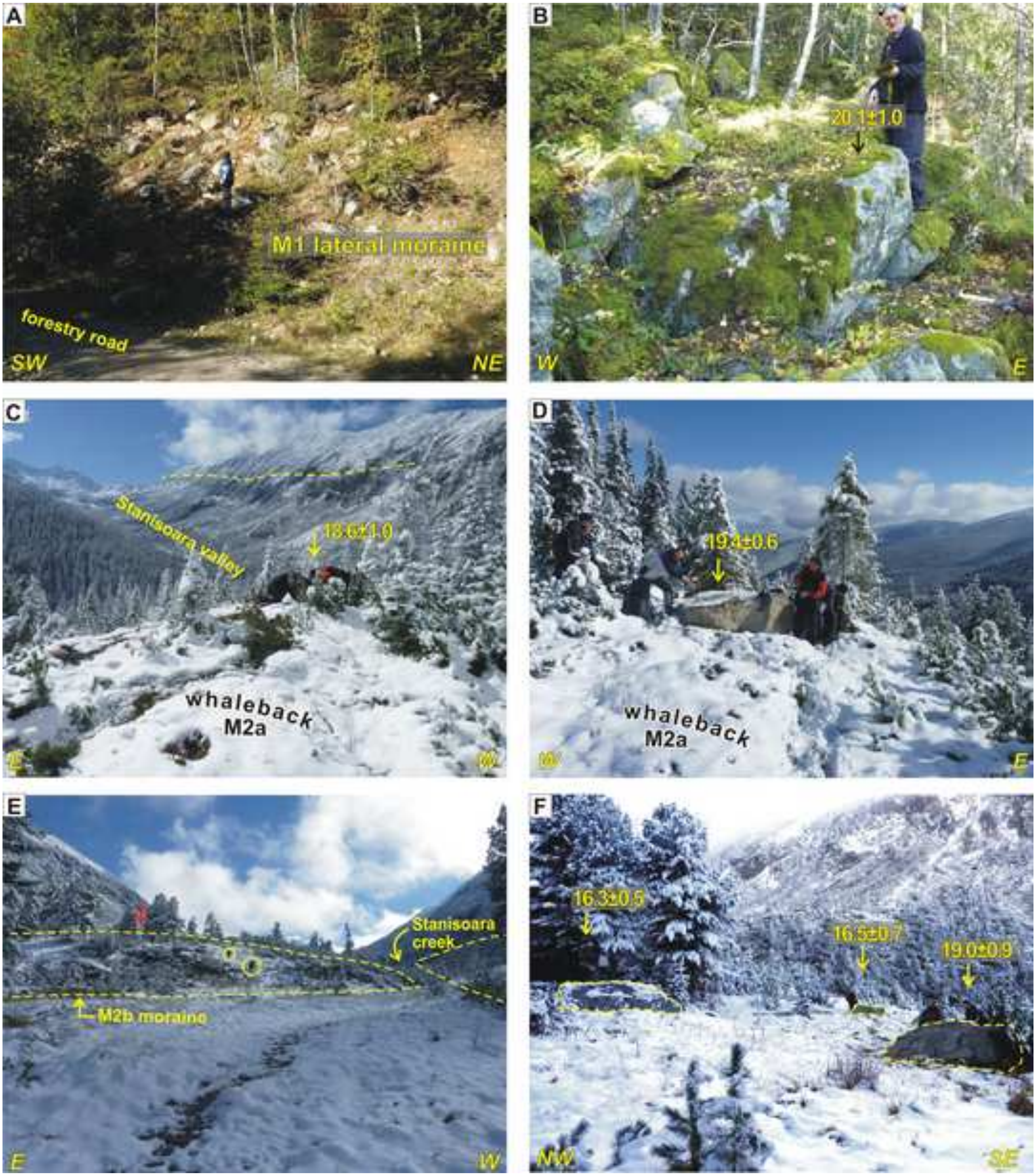

Figure 4
Click here to download high resolution image

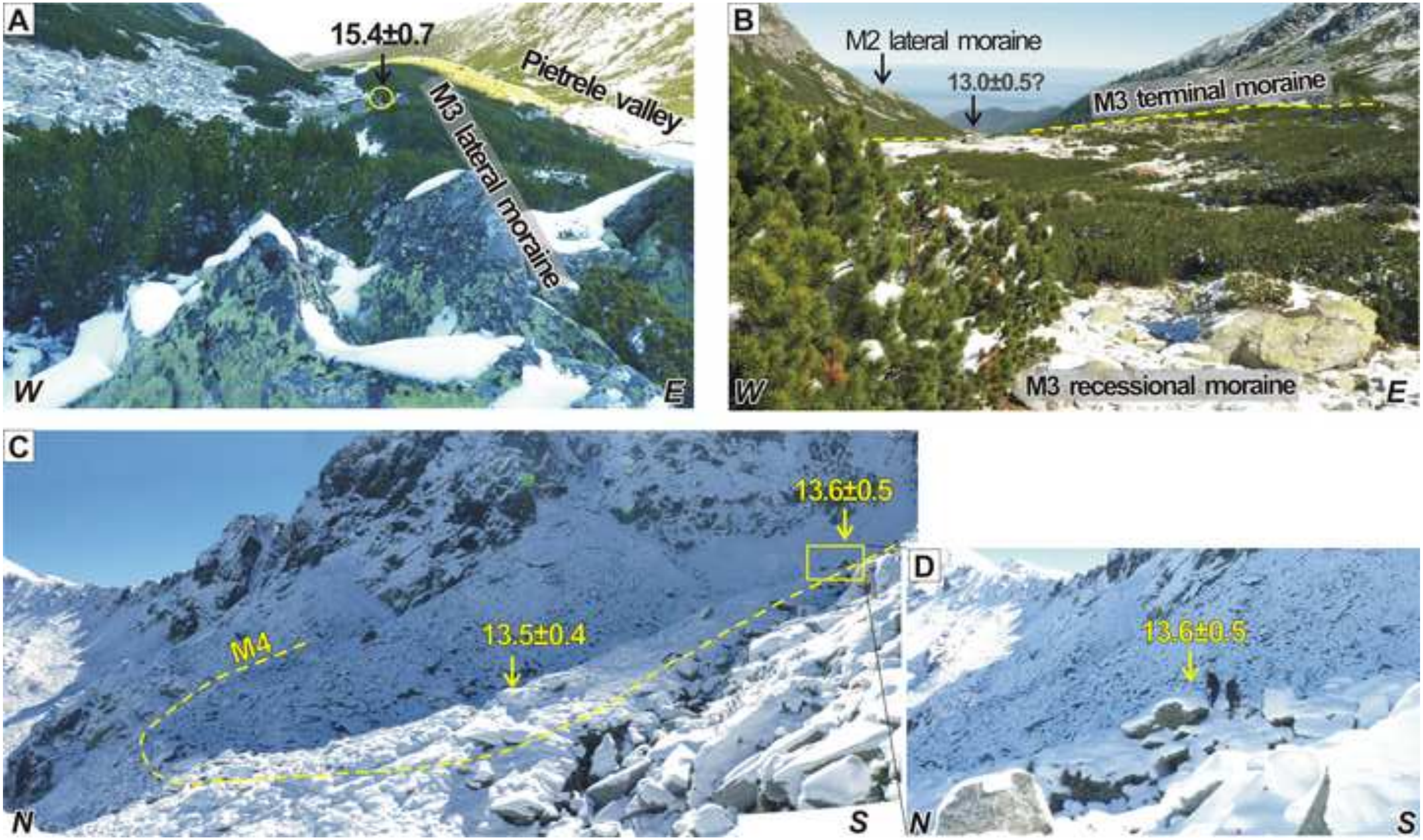

Figure 5

Click here to download high resolution image

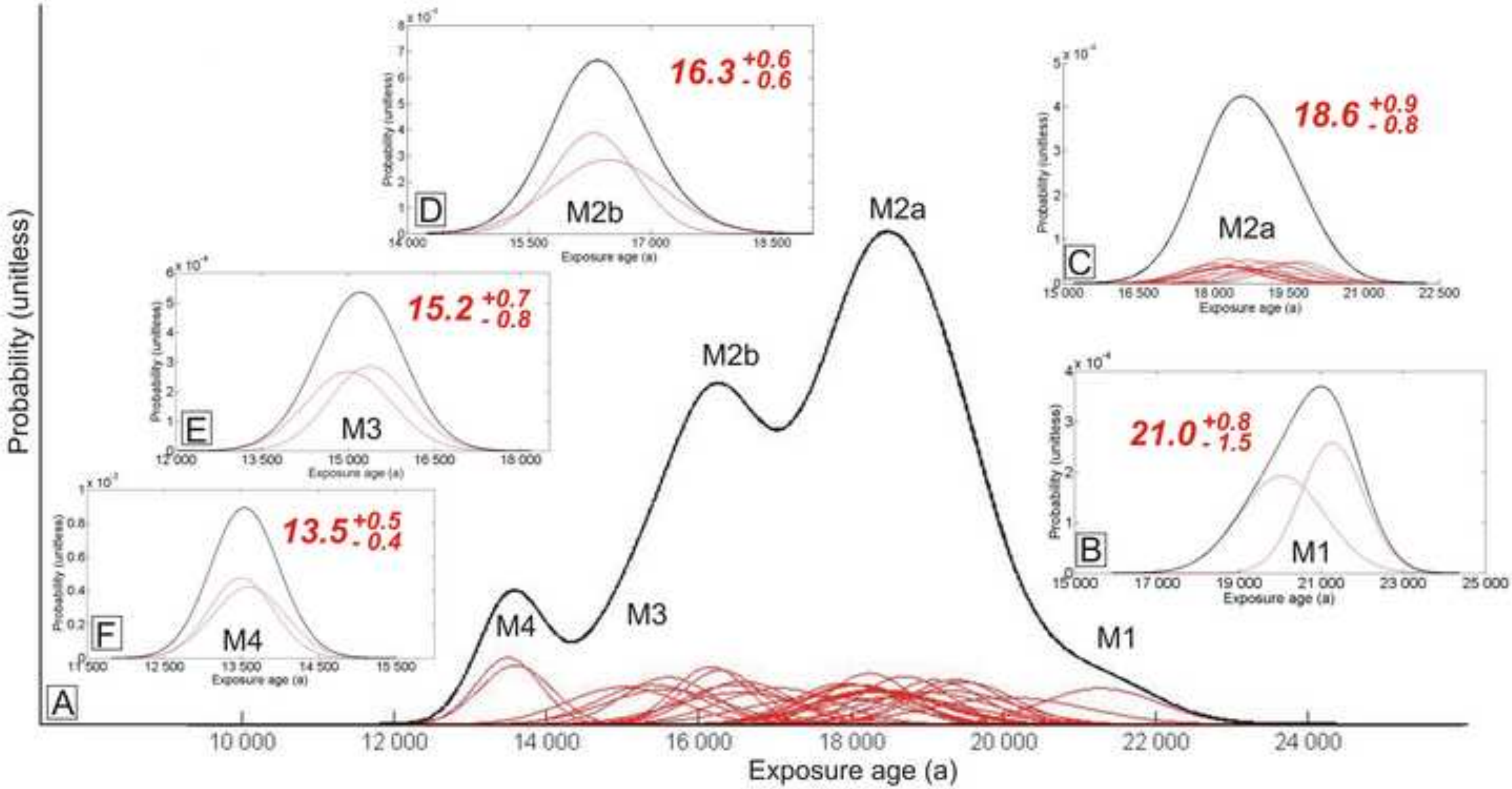

Figure 6
Click here to download high resolution image

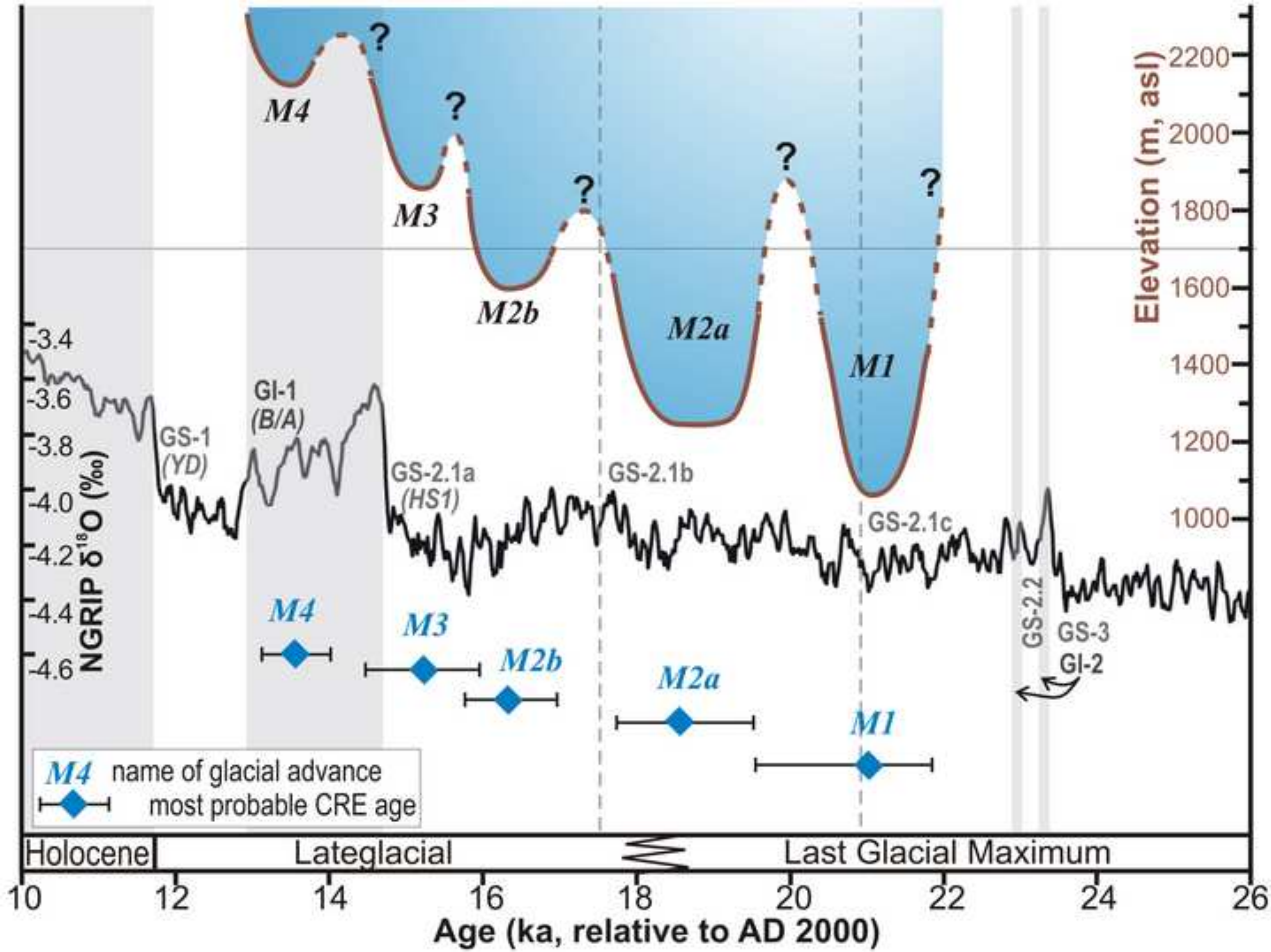

**Table**

| Sample | Location | Latitude (DD) | Longitude (DD) | Elevation (m) | Thickness (cm) | Boulder size* (cm) | Strike/dip (°) | Self shielding | Topo shielding | Snow shielding | Soil shielding |
|---|---|---|---|---|---|---|---|---|---|---|---|
| **Re13-01** | erratic b. | 45.4007 | 22.8668 | 1752 | 1.0 | 100x285x190 | 0 | 0.992 | 0.987 | 0.969 | 1.00 |
| **Re13-02** | whaleback | 45.4007 | 22.8668 | 1748 | 1.5 | - | 0 | 0.987 | 0.987 | 0.969 | 1.00 |
| **Re13-03** | erratic b. | 45.4007 | 22.8668 | 1750 | 1.0 | 160x200x190 | 0 | 0.992 | 0.987 | 0.969 | 1.00 |
| **Re13-04** | lat. mor. | 45.4009 | 22.8660 | 1771 | 1.5 | 90x375x130 | 275/10 | 0.987 | 0.983 | 0.969 | 1.00 |
| **Re13-05** | lat. mor. | 45.4009 | 22.8660 | 1769 | 1.0 | 80x350x180 | 130/15 | 0.992 | 0.982 | 0.969 | 1.00 |
| **Re13-06** | t. mor. | 45.3945 | 22.8639 | 1770 | 3.0 | 120x420x130 | 0 | 0.975 | 0.969 | 0.945 | 1.00 |
| **Re13-07** | t. mor. | 45.3945 | 22.8639 | 1770 | 3.0 | 140x330x250 | 0 | 0.975 | 0.969 | 0.945 | 1.00 |
| **Re13-08** | t. mor. | 45.3945 | 22.8639 | 1770 | 2.0 | 90x255x220 | 0 | 0.983 | 0.969 | 0.945 | 1.00 |
| **Re13-09** | t. mor. | 45.3708 | 22.8664 | 2150 | 2.0 | 120x370x310 | 60/15 | 0.983 | 0.948 | 0.917 | 1.00 |
| **Re13-10** | t. mor. | 45.3710 | 22.8671 | 2138 | 1.0 | 55x150x60 | 0 | 0.992 | 0.958 | 0.917 | 1.00 |
| **Re13-11** | lat. mor. | 45.3744 | 22.8702 | 2036 | 1.0 | 160x400x300 | 190/7 | 0.992 | 0.985 | 0.927 | 1.00 |
| **Re13-12** | lat. mor. | 45.3748 | 22.8706 | 2024 | 2.5 | 350x1500x250 | 0 | 0.979 | 0.993 | 0.927 | 1.00 |
| **Re13-13** | lat. mor. | 45.4278 | 22.8959 | 1124 | 1.0 | 120x340x310 | 0 | 0.992 | 0.963 | 0.982 | 0.986 |
| **Re13-14** | lat. mor. | 45.4283 | 22.8957 | 1122 | 1.0 | 140x330x230 | 140/20 | 0.992 | 0.958 | 0.982 | 0.994 |
| **Re13-15** | lat. mor. | 45.4281 | 22.8960 | 1106 | 1.0 | 160x280x240 | 80/15 | 0.992 | 0.961 | 0.982 | 0.983 |

Table 1. Location of sample sites and correction factors used for the CRE age calculation. *Boulder size is given as “height x length x width”; lat. mor: lateral moraine; t. mor : terminal moraine.

**Table**

| Sample | Glacier advance* | [$^{10}$Be] concentration (at/g $SiO_2$) | | | CRE age (a) no uplift, no denudation | | | CRE age (a) uplift=1mm/a, denudation=3mm/ka | | | CRE age (a) as published by Reuther et al. (2007) uplift=3.5mm/a, denudation=5mm/ka | | |
|---|---|---|---|---|---|---|---|---|---|---|---|---|---|
| **Re13-01** | M2a | 292 586 | ± | 9 459 | 18 310 | ± | 592 | 19 364 | ± | 626 | - | | - |
| **Re13-02** | M2a | 279 510 | ± | 15 399 | 17 613 | ± | 970 | 18 581 | ± | 1 024 | - | | - |
| **Re13-03** | M2a | 282 832 | ± | 8 780 | 17 723 | ± | 550 | 18 703 | ± | 581 | - | | - |
| **Re13-04** | (M2a) | 210 521 | ± | 18 559 | 13 079 | ± | 1 153 | 13 601 | ± | 1 199 | - | | - |
| **Re13-05** | (M2a) | 269 907 | ± | 15 332 | 16 769 | ± | 953 | 17 643 | ± | 1 002 | - | | - |
| **Re13-06** | M2b | 237 291 | ± | 7 506 | 15 553 | ± | 492 | 16 297 | ± | 516 | - | | - |
| **Re13-07** | (M2b) | 274 078 | ± | 12 565 | 17 975 | ± | 824 | 18 981 | ± | 870 | - | | - |
| **Re13-08** | M2b | 241 726 | ± | 10 294 | 15 712 | ± | 669 | 16 472 | ± | 701 | - | | - |
| **Re13-09** | M4 | 250 216 | ± | 8 689 | 13 084 | ± | 454 | 13 602 | ± | 472 | - | | - |
| **Re13-10** | M4 | 251 016 | ± | 7 798 | 12 988 | ± | 403 | 13 499 | ± | 419 | - | | - |
| **Re13-11** | M3 | 269 023 | ± | 13 376 | 14 386 | ± | 715 | 15 018 | ± | 747 | - | | - |
| **Re13-12** | M3 | 271 623 | ± | 12 357 | 14 720 | ± | 670 | 15 382 | ± | 700 | - | | - |
| **Re13-13** | M1 | 193 219 | ± | 7 017 | 20 000 | ± | 726 | 21 271 | ± | 773 | - | | - |
| **Re13-14** | M1 | 183 170 | ± | 9 462 | 18 919 | ± | 977 | 20 053 | ± | 1 036 | - | | - |
| **Re13-15** | (M1) | 144 244 | ± | 7 962 | 15 193 | ± | 839 | 15 912 | ± | 878 | - | | - |
| **RT-03-01** | M2a | 224 450 | ± | 8 754 | 17 232 | ± | 672 | 18 105 | ± | 706 | 15 900 | ± | 530 |
| **RT-03-02** | (M2a) | 194 341 | ± | 7 385 | 14 957 | ± | 568 | 15 604 | ± | 593 | 13 800 | ± | 460 |
| **RT-03-03** | M2a | 222 626 | ± | 10 018 | 17 444 | ± | 785 | 18 340 | ± | 825 | 16 100 | ± | 620 |
| **RT-03-04** | M2a | 238 136 | ± | 10 240 | 18 309 | ± | 787 | 19 303 | ± | 830 | 16 800 | ± | 620 |
| **PT-03-04** | (M2a) | 211 677 | ± | 11 219 | 15 814 | ± | 838 | 16 541 | ± | 877 | 14 600 | ± | 670 |
| **PT-03-05** | (M2a) | 209 852 | ± | 9 443 | 16 270 | ± | 732 | 17 043 | ± | 767 | 15 000 | ± | 590 |
| **PT-03-07** | M2a | 239 049 | ± | 7 889 | 18 124 | ± | 598 | 19 096 | ± | 630 | 16 700 | ± | 470 |
| **PT-03-08** | M2a | 228 100 | ± | 10 036 | 17 404 | ± | 766 | 18 295 | ± | 805 | 16 000 | ± | 610 |
| **PT-03-09** | M2a | 232 662 | ± | 10 470 | 17 546 | ± | 790 | 18 453 | ± | 830 | 16 200 | ± | 630 |
| **PT-03-10** | M2a | 231 750 | ± | 10 892 | 17 443 | ± | 820 | 18 338 | ± | 862 | 16 100 | ± | 650 |
| **PT-03-20** | M2a | 248 173 | ± | 9 679 | 17 171 | ± | 670 | 18 035 | ± | 703 | 15 900 | ± | 530 |
| **PT-03-21** | (M2a) | 215 326 | ± | 6 460 | 15 468 | ± | 464 | 16 161 | ± | 485 | 14 300 | ± | 380 |
| **PT-03-11** | (M2a) | 197 991 | ± | 10 098 | 14 927 | ± | 761 | 15 570 | ± | 794 | 13 800 | ± | 620 |
| **PT-03-12** | M2a | 236 312 | ± | 7 089 | 17 356 | ± | 521 | 18 242 | ± | 547 | 16 000 | ± | 410 |
| **PT-03-13** | (M2a) | 209 852 | ± | 8 184 | 15 849 | ± | 618 | 16 579 | ± | 647 | 14 700 | ± | 500 |
| **SA-03-01** | M2a | 279 194 | ± | 9 493 | 18 484 | ± | 628 | 19 491 | ± | 663 | 16 400 | ± | 480 |
| **PT-03-16** | (M2a-b) | 337 588 | ± | 12 828 | 17 069 | ± | 649 | 17 917 | ± | 681 | 16 000 | ± | 520 |
| **PT-03-02** | (M3) | 218 064 | ± | 8 286 | 12 560 | ± | 477 | 13 003 | ± | 494 | 11 400 | ± | 390 |
| **PT-03-03** | (>M3) | 251 822 | ± | 9 066 | 15 023 | ± | 541 | 15 673 | ± | 564 | 13 600 | ± | 430 |

Table 2. Results of $^{10}$Be CRE age measurements and calculated CRE ages.

Shielding corrections and site specific spallogenic production rates were calculated using CosmoCalc (Vermeesch, 2007) and scaling factors of Stone (2000) and the SLHL production rate of 4.02±0.36 atoms/gr$SiO_2$/yr, the weighted mean of recently calibrated production rates in the Northern Hemisphere (Balco et al., 2009; Fenton et al., 2011; Goehring et al., 2012; Briner et al., 2012). $^{10}Be/^{9}Be$ ratios of process blanks were $(1.43 \pm 0.4) \times 10^{-15}$.

*Codes in brackets indicate samples discarded from the calculation of the most probable CRE age of the relevant glacier advance. See details in the text.